

Organization of Dorsal Cochlear Nucleus Type IV Unit Response Maps and Their Relationship to Activation by Bandlimited Noise

GEORGE A. SPIROU AND ERIC D. YOUNG

Department of Biomedical Engineering and Center for Hearing Sciences, The Johns Hopkins University School of Medicine, Baltimore, Maryland 21205

SUMMARY AND CONCLUSIONS

1. Response maps of 49 type IV neurons in cat dorsal cochlear nucleus (DCN) were studied by moving a tone in small steps along the frequency dimension and along the intensity dimension. Type IV responses are recorded from DCN principal cells. Data were collected from 38 units with best frequencies (BFs) from 2.16 to 50.3 kHz with the use of electrode penetrations along the long (strial) axis of the DCN; an additional 11 units from a previous study were analyzed. A stereotypical type IV response map is defined as consisting of two excitatory and two inhibitory regions. Type IV units from both the pyramidal cell layer (probably pyramidal cells) and the deep layer (probably giant cells) show the same types of response maps.

2. Two of the regions, one excitatory and one inhibitory, are seen in all type IV units. These regions are a low-threshold excitatory region at best frequency (BFER) and an inhibitory area at higher levels, usually centered below BF but extending upward in frequency to include BF (central inhibitory area, or CIA). The high resolution of the response maps in this paper allows us to show that type IV units fall into two groups on the basis of whether their CIAs are narrow with well-defined borders (35 units) or broad with poorly defined borders (14 units).

3. Two additional features of type IV response maps can be defined, most consistently in units with well-defined CIAs. These features are an excitatory region along the high-frequency edge of the CIA (upper excitatory region, UER) and an upper inhibitory sideband (UIS). The BFER and UER are continuous in many units, but in some cases their continuity is broken by the CIA. It seems likely that the BFER and UER represent a single excitatory input to type IV units and are revealed because the tuning curve of the stronger inhibitory inputs that produce the CIA has thresholds greater than and BFs lower than the excitatory inputs.

4. The CIA is probably produced by inhibitory inputs from DCN type II neurons. The bandwidths of type IV CIAs are about 1–3 times larger (at 40 dB above threshold) than the excitatory bandwidths of DCN type II units, suggesting a convergence of the equivalent in tuning of about two type II units onto each type IV unit. The BF of the CIA is below the excitatory BF of the type IV unit in most cases.

5. Responses of type IV units to notch noise, which is band-reject filtered noise with the center of the stop band placed at BF, were recorded. Plots of discharge rate versus notch width were constructed with the use of these data. These plots show excitatory responses to noise with narrow notches (less than a few kilohertz for units with BFs >10 kHz) and inhibitory responses to noise with wider notches.

6. Units' response maps are used to generate predicted responses to notch noise signals, with the result that the responses of DCN neurons to the notch noise cannot be explained by a model in which stimulus energy in different frequency bands is weighted according to the response map and summed to produce the unit's output (quasilinear energy summation). The model predictions

for narrow notches are usually the inverse of the actual responses of the units. However, the notch noise responses are consistent with response map features to the limited extent that there is a general correspondence between the width of the BFER a few decibels above threshold and the notch width at which the excitatory responses disappear. The notch noise data point up the fundamental nonlinearity of energy summation in DCN units and demonstrate the need for more sophisticated analysis of input-output relationships in this structure. These results can be explained, at least qualitatively, in terms of preliminary results on the organization of response maps in type II units.

INTRODUCTION

The cochlear nucleus (CN) contains a number of subnuclei that differ from one another in terms of cytoarchitecture (Brawer et al. 1974; Lorente de Nò 1981; Osen 1969; Ramón y Cajal 1909), connectivity with other auditory system nuclei (Cant and Morest 1984; Warr 1982), and physiological characteristics of responses to sound (Evans and Nelson 1973a; Young 1984). The dorsal cochlear nucleus (DCN) has the most intricate interneuronal organization and synaptic structure among the CN subdivisions (Kane 1974; Lorente de Nò 1981; Mugnaini et al. 1980a; Osen et al. 1990). DCN responses to sound differ dramatically from those of auditory nerve fibers and apparently reflect a balance of excitatory and inhibitory influences from multiple sources (Evans and Nelson 1973a,b; Greenwood and Maruyama 1965; Rhode and Kettner 1987; Shofner and Young 1987; Voigt and Young 1980, 1990).

Unlike neurons in the ventral CN, DCN units do not display temporal patterns of response to sound (chopping, pausing, etc.) that are characteristic of cell type; instead, individual units may display several patterns, depending on stimulus parameters (Godfrey et al. 1975; Rhode and Kettner 1987). Moreover, classification of DCN units on the basis of temporal patterns of response to sound does not seem to distinguish classes of units that are clearly differentiated in terms of other response properties (Shofner and Young 1985). However, comprehensive DCN unit classes can be defined on the basis of response maps (plots of discharge rate over a range of sound levels and frequencies) and responses to broadband noise stimuli (Young and Brownell 1976; Young and Voigt 1982). The resulting classification scheme divides units into types I–V in order of increasing dominance of their response maps by inhibition (Evans and Nelson 1973a; Young and Brownell 1976).

Units with the most inhibition in their response maps

(types IV and V) can also be activated antidromically from the dorsal acoustic stria (Young 1980) and are therefore presumed to be DCN principal cells (Adams and Warr 1976). A second group, type II units, is characterized by a number of features, the most prominent of which is their weak response to broadband stimuli (Young and Voigt 1982). Type II units can sometimes be activated antidromically from the anteroventral division of the CN (AVCN; Young 1980); therefore we assume that they are recorded from an apparently glycinergic interneuron in the deep layer of the DCN, the vertical cell, the axon of which gives a collateral to the AVCN (Lorente de Nò 1981; Oertel and Wu 1989; Osen et al. 1990; Saint Marie et al. 1991). Type II units have been shown by cross-correlation analysis (Voigt and Young 1980, 1990) to inhibit type IV units in the DCN, and vertical cells have been shown to inhibit ventral CN (VCN) principal cells (Wickesberg and Oertel 1988, 1990).

A distinguishing feature of type IV neurons is the dichotomous nature of their responses to narrowband versus broadband sounds. Tone bursts at best frequency (BF) yield an inhibitory response for a range of sound levels, whereas broadband noise usually yields an excitatory response at the same sound levels (Young and Brownell 1976). The difference between responses to narrowband and broadband stimuli can be explained in terms of the properties of the inhibitory input from type II units (Young 1984; Young and Brownell 1976). Type II units give strong responses to tones but weak responses to broadband stimuli (Young and Voigt 1982).

In this study, we have examined in more detail the relationship between responses of DCN type IV units to broadband and to narrowband stimuli. We show that the response maps of most DCN type IV units have stereotypical features that can be related to the presumed topography of their inhibitory innervation by type II units. As a broadband stimulus, we use notch noise, which is broadband noise (BBN) from which energy has been removed at frequencies in a band centered on the BF of the unit under study, creating a notch in the noise spectrum. By recording the change in response of the unit as the notch width is changed, we can define the response contributed by noise components in a particular frequency region. This method is similar to psychophysical methods for determining auditory filter shape (Patterson 1976). A comparison of noise responses defined in this way to tone responses at the same frequencies clearly demonstrates the fact that responses to noise cannot be predicted from responses to tones, i.e., from response maps. However, the responses to notch noise stimuli can be explained in terms of the properties of type II units and the organization of their connections to type IV units.

METHODS

Animal preparation and unit recording

Sixteen adult cats (1.8–3.6 kg), selected to have clean external ears, translucent tympanic membranes, and no signs of middle ear infection, were used in these experiments. Additional data were taken from seven animals from a previously reported study (Voigt and Young 1990). Animals were injected with 0.1 mg atropine to

control mucus secretions and anesthetized with an intramuscular injection of 100–120 mg ketamine. After a tracheotomy, each animal was placed in a head holder in an electrically shielded soundproof room (IAC-1204A). Body temperature was maintained at 36–38°C with the use of a heating pad. An opening was made in the bone over the left parietal cortex; the cortex and caudal hippocampus were aspirated to reveal the midbrain and caudal thalamus. Decerebration was performed by aspiration through the rostral superior colliculus under visual control. No anesthetic was given after decerebration. An intraperitoneal injection of 10 ml physiological saline was given to help preserve fluid volume. The external meati of both ears were exposed and transected, and the animal was mounted in a stereotaxic frame supported by hollow ear bars and a metal plate attached to the frontal bone. To equalize pressure on the tympanic membrane, we vented the bulla by boring a small hole in it with an awl and inserting a 60-cm length of PE-200 tubing. No drilling was performed on the bulla.

The skull was opened over the midline cerebellum. Cerebellar tissue was removed, exposing the floor of the fourth ventricle. The contralateral DCN and restiform body were exposed to serve as landmarks for exposing the ipsilateral DCN. Cerebellar tissue was aspirated over the dorsomedial portion of the ipsilateral DCN, carefully avoiding damage to the choroid plexus. In two animals, the DCN was exposed with the use of a caudal approach, which requires no aspiration of neural tissue (see Shofner and Young 1985).

Platinum-iridium microelectrodes were used to record single units. The electrodes were positioned initially at the dorsomedial edge of the DCN and oriented parallel to its surface (35–40° from vertical). Electrodes traveled from dorsomedial to ventrolateral and crossed the tonotopic axis, from frequencies >30 kHz down to a few kilohertz. The tonotopy of the nucleus makes the tuning of high-BF units more reliable, as exemplified by the 50.3-kHz unit shown in Fig. 3C. To achieve stability, we infiltrated the exposure with a wax-mineral oil mixture that had a melting point of ~38°C. Most of the plug hardened, providing a hydraulic seal of the exposure. For greater recording stability, some animals were artificially respiration after a pneumothorax. These animals were paralyzed with an injection of gallamine triethiodide (Flaxedil IV; 20 mg), with supplemental doses (10 mg) every few hours.

Acoustic stimuli

Pure tones, BBN, and notch noise were the stimuli used in these experiments. All stimuli were 200 ms long with 10-ms rise/fall times and a 1-s repetition period, except for those used in constructing response maps, which were 150 ms long with a 1-s period. A shorter stimulus duration was used for response map data to reduce the effects of offset inhibition on the response to the next stimulus presentation (Rhode et al. 1983; Rhode and Smith 1986). Sound was delivered from an electrostatic driver to the ipsilateral ear through a hollow ear bar (Sokolich 1977). Acoustic calibrations at the eardrum were done with a probe tube for each animal. Examples of calibration curves are shown above response maps in Figs. 11 and 12.

Notch noise stimuli were generated by band-pass filtering two independent BBNs (from Elgenco model 3602 noise generators) at 24 dB/octave, with low cutoff f_l and high cutoff f_h . The filtered noises were multiplied by quadrature tones at the desired center frequency of the notch (i.e., one by $\cos 2\pi f_0 t$, the other by $\sin 2\pi f_0 t$) and the outputs of the multipliers were added, thereby creating stationary band-reject noise centered at frequency f_0 . The bandwidth of the notch is $2f_0$ and the total bandwidth of the noise is $2f_h$. When properly balanced, the level of the carrier tone at the center of the notch was ≥20 dB below the spectrum level of the noise. Examples of band-reject stimuli centered at 20 kHz are

shown in Fig. 1 for notch widths ($2f_1$) of 2, 8, and 12 kHz. The noise floor for these stimuli is 20–30 dB below the passband. The spectra roll off at frequencies >40 kHz because the f_h of the original bandpass filter was set at 20 kHz.

Experimental protocol

Tones at the BF of the unresolved neural background activity from the electrode were used to search for units. When a unit was isolated, its BF and threshold were determined manually. Rate-level series for responses to BF tones and BBN were collected, covering a 100-dB range in 1-dB increments. On the basis of these data, the unit's response type (type II, III, or IV) was determined by the criteria described in Young (1984). Next, the unit's response map was generated with the use of tonal stimuli. Tones were stepped across a frequency range (logarithmically in 100 steps) at constant attenuation, with one repetition at each frequency. At the highest sound levels, the frequencies ranged from ~2 octaves below to 1 octave above BF. Attenuations were usually changed in 10-dB increments, although, near threshold, smaller increments were often used. A range of 80–90 dB was covered in most units. Response maps for 11 units taken from an earlier study (Voigt and Young 1990) were assembled from data taken with a different protocol: in this case, rate-level curves were determined for tones covering as much as a 100-dB range, in 2-dB increments, at frequencies spaced at 0.1- or 0.2-octave intervals.

Response maps (for example, Fig. 2) are constructed off line. Driven and spontaneous rates are computed over windows of 10–150 and 800–990 ms respectively, relative to stimulus onset. Response maps are plotted as discharge rate versus frequency at a succession of constant attenuations (data from frequency steps) or at a succession of constant SPLs (data from rate-level curves). Slow variations in discharge rate that occur equally in driven and spontaneous rates were sometimes seen; these variations are controlled by subtracting the spontaneous rate from the driven rate at each point in the response map. The resulting rate differences are

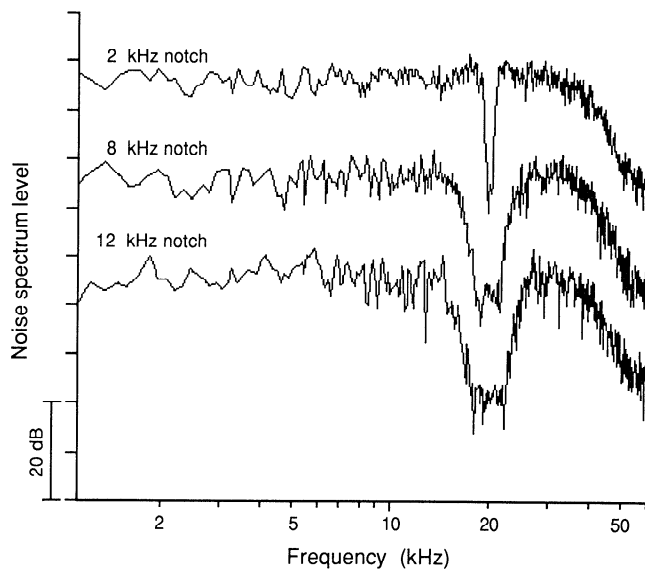


FIG. 1. A: examples of notch noise stimuli. Notch widths of 2, 8, and 12 kHz are shown, centered on 20 kHz. The 8-kHz notch has a bump in the floor of the notch, which reflects the energy at the carrier frequency. Spectra are separated by 20 dB along the ordinate for clarity. Falloff in notch noise spectra above 40 kHz reflects the upper cutoff frequency of the noise (f_h) before multiplying by the carrier. These are spectra of the electrical signal at the input to the earphone; they are modified by acoustic system transfer functions (e.g., Figs. 11 and 12) when presented in experiments.

smoothed with the use of a triangular filter 3 bins wide. Rate-level data are converted to rate-versus-frequency form for plotting after the rate-differencing and -smoothing operations. An average spontaneous rate at each sound level is computed from the first 12 stimuli, which are usually outside of the regions of excitation and inhibition. In the response map, the average spontaneous rate is plotted as a horizontal straight line at each sound level. Rate differences (rate minus spontaneous rate) are plotted with this line as zero, so excitatory responses are above the line and inhibitory responses are below it.

Excitation and inhibition are marked by hand in response maps at frequencies at which rate falls above or below spontaneous rate and appears continuous with similar responses at adjacent frequencies. Areas of weak excitation and inhibition may be missed unless they are part of a larger region of the response map.

After response map data were taken, notch noise series were presented. Data were taken as rate-versus-level functions for a series of notch noise stimuli. Usually, notch widths were varied in 1-kHz increments from 1 to 10 kHz, then in 2-kHz increments from 10 to 20 kHz. Between each series of stimuli, BF tone and BBN rate-level curves were obtained to verify stability of the unit.

Stimulus levels are given as dB SPL (decibels re 20 μPa) in response maps constructed from rate-level curves, as decibels of attenuation in response maps constructed from frequency steps (0 dB attenuation is approximately 100 dB SPL for frequencies <25 kHz), or as noise spectrum level in the passband for noise rate-level curves. Noise spectrum level is the energy in a 1-Hz band at unit BF and at the level of the noise passband and is specified in units of decibels re 20 $\mu\text{Pa}/\sqrt{\text{Hz}}$.

Histology

Although type IV responses have been associated with DCN principal cells, we were interested in differentiating recordings made in the pyramidal cell layer from recordings made in deep layers because of the different synaptic organization in these regions. Electrolytic lesions (15 μA for 15–30 s) were made at the end of the final track in each animal. Because of the length of electrode tracks (up to 5 mm), few penetrations were made (6 animals had only 1 electrode track). Before perfusion, animals were injected intravenously with 1–2 ml heparin to prevent blood clotting and anesthetized with pentobarbital sodium (25–50 mg iv). The animals were perfused transcardially with 0.9% NaCl followed by 10% formal-saline. Their brains were removed; and, after several days in fixative, the regions containing the CNs were frozen, sectioned in the transverse plane at 48 μm , and stained with cresyl violet. Microdrive micrometer readings were associated with lesion sites so that units could be localized to either the pyramidal cell layer or deep regions of the nucleus (see Table 1). Many units could not be localized because they were not isolated along the final track in an experiment or because the electrode track was not recovered.

RESULTS

Type IV response maps

The results in this paper are based on response maps of 49 type IV units, including 11 type IV units from an earlier study (Voigt and Young 1990), the BFs of which cover the range from 2.16 to 50.3 kHz. Examples of response maps are shown in Figs. 2 and 3. In these response maps, inhibitory areas are stippled and excitatory areas are solidly filled. Vertical bars at the top of each plot indicate the unit's BF. These bars make clear the nonmonotonicity of BF rate-

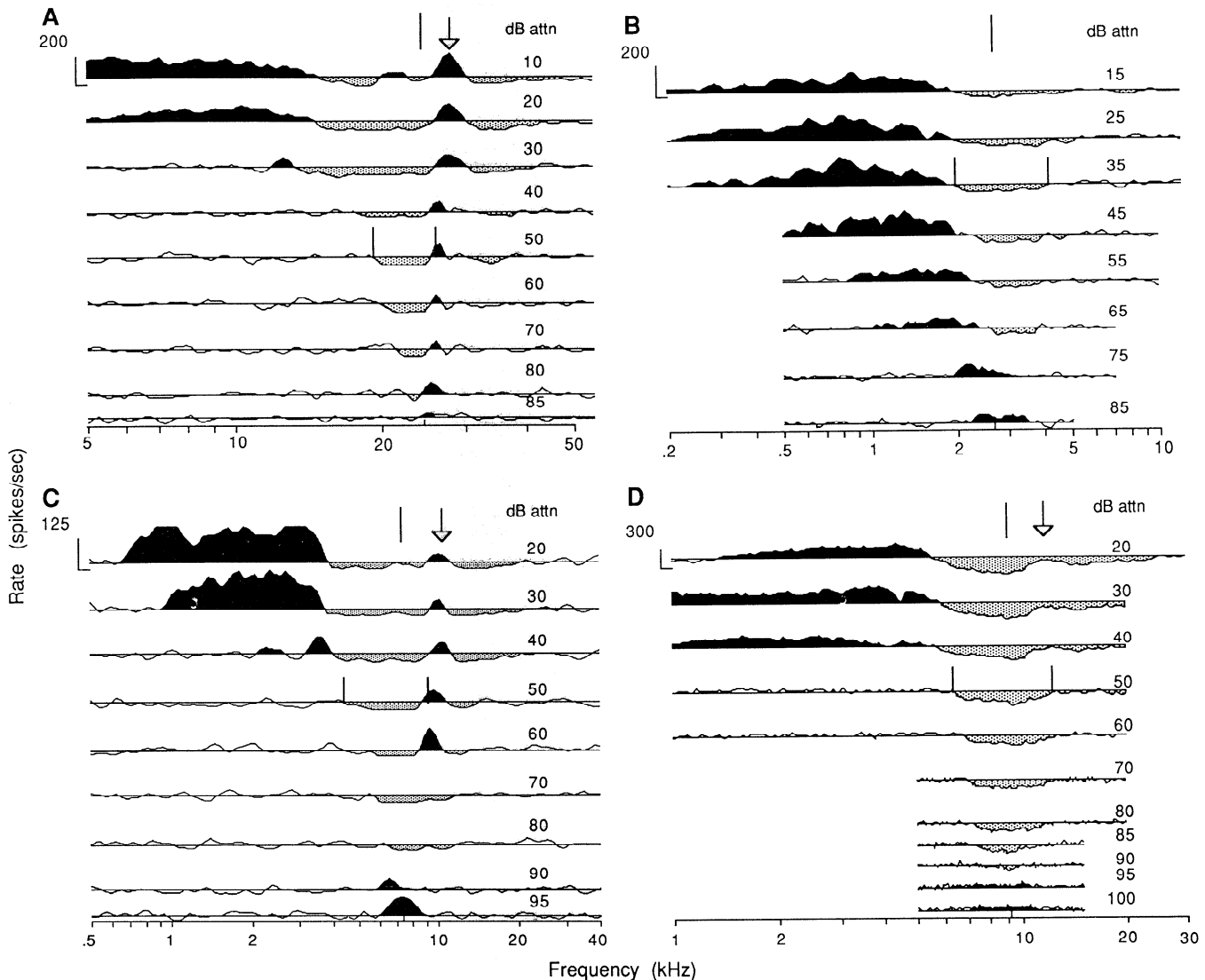


FIG. 2. Response maps of 4 type IV units that exhibit standard features of organization. Scale bar for rate shown at top left on each response map. Length of bar corresponds to the rate indicated at left of the bar; horizontal line at bottom of bar shows where rate equals zero. Stippled areas indicate inhibition; solid areas indicate excitation. BF is marked with a vertical line at the top of each plot. Open arrows at top of A, C, and D mark excitation (UER) at high-frequency edge of CIA. Pairs of vertical lines indicate edges of CIA at 30–40 dB above inhibitory threshold. Sound levels are shown as decibels of attenuation; actual sound pressure level varies with acoustic calibration, but 0 dB attenuation is usually near 100 dB SPL. A: BF 21.3 kHz, spontaneous rate 39.0 spikes/s, CIA Q₄₀ 2.32, pyramidal cell layer. B: BF 2.64 kHz, spontaneous rate 33.5 spikes/s, CIA Q₄₀ 1.06, not localized. C: BF 7.41 kHz, spontaneous rate 17.3 spikes/s, CIA Q₄₀ 1.40, deep layer. D: BF 9.2 kHz, spontaneous rate 62.7 spikes/s, CIA Q₄₀ 1.46, deep layer.

level curves that is characteristic of type IV units (Young and Brownell 1976). The response is excitatory near BF threshold but enters an inhibitory area within 30 dB of threshold. The response maps in Fig. 2 exemplify the majority of our sample (35/49) in that they are composed of four

standard features. These features are shown schematically in Fig. 4 and are discussed below. The units in Fig. 3 show some, but not all, of the standard features and are included to illustrate the range of response maps we have encountered.

The first feature of typical type IV response maps is a low-level excitatory region at BF (BFER). This excitatory area begins at BF threshold and extends to higher levels. It is present in almost all type IV units; when it is missing, the unit is called type V (Evans and Nelson 1973a), but we find few such units. The BFER is seen as an isolated entity in Figs. 2C (95 and 90 dB attenuation) and 3D (110–100 dB attenuation), where it is separated from other excitatory regions by inhibitory areas. The excitation at BF can be very subtle, as in Fig. 3D, and may not exhibit large driven

TABLE 1. Type IV response map categories and localization of units

	Total	Pyramidal Cell Layer	Deep layer	Not localized
Well-defined CIA	35	14	5	16
Poorly defined CIA	14	5	1	8
Total	49	19	6	24

CIA, central inhibitory layer.

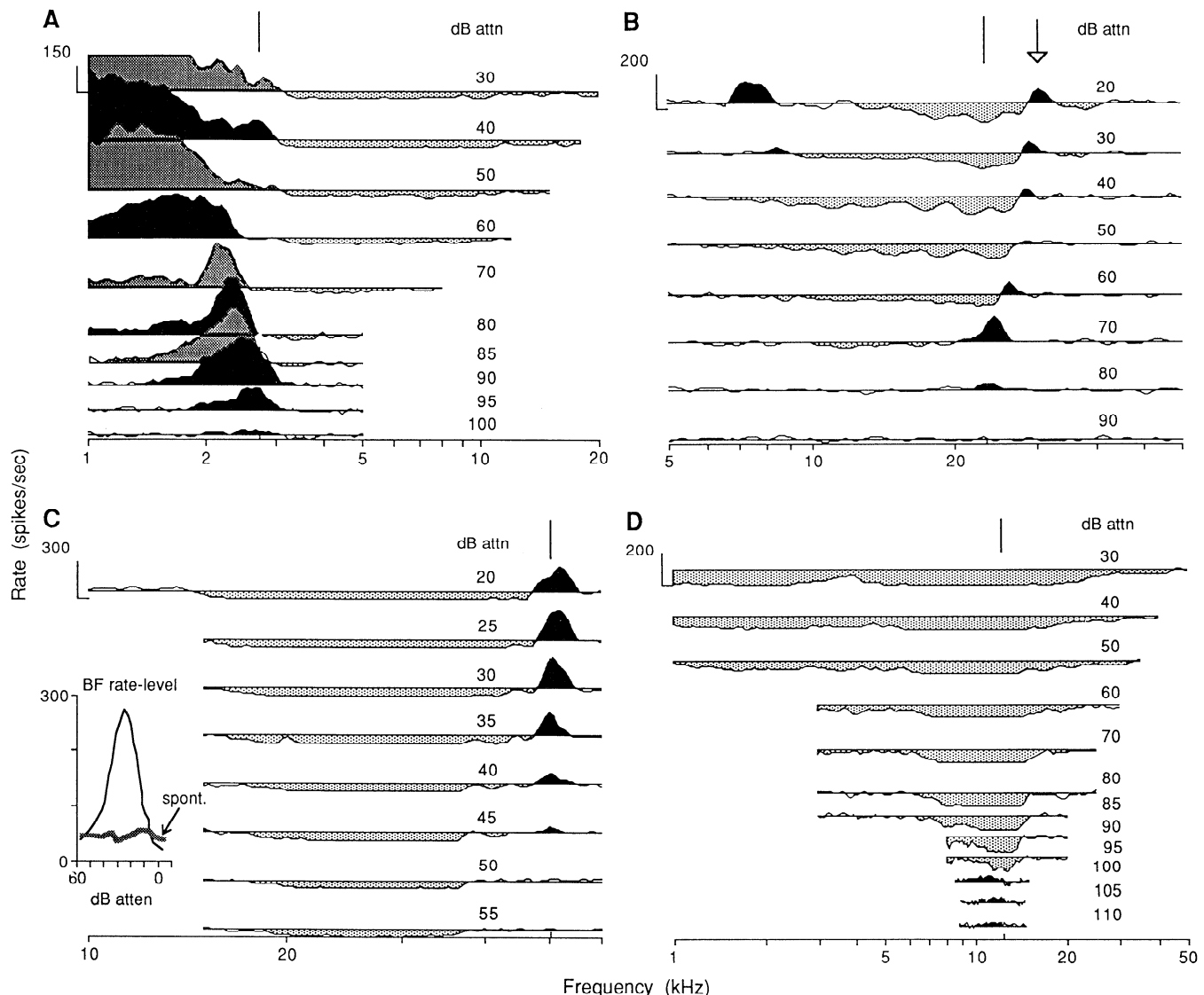


FIG. 3. Response maps of 4 type IV units that do not fit the standard organization scheme. All units are type IV in that they are excited by low-level sounds and have central inhibitory areas. However, their central inhibition is broad in frequency and lacks well-defined upper and/or lower bounds. *A*: BF 2.75 kHz, spont rate 5.3 spikes/s, pyramidal cell layer. *B*: BF 23.4 kHz, spont rate 13.3 spikes/s, pyramidal cell layer. *C*: BF 50.3 kHz, spont rate 43.5 spikes/s, pyramidal cell layer. Inset: rate-level curve at 50.3 kHz that shows the nonmonotonicity typical of type IV units at BF. CIA is inferred for this unit because stimuli at sufficiently high levels could not be produced at unit's BF. *D*: BF 12.4 kHz, spont rate 97.1 spikes/s, not localized.

rates. Generally, rates do not exceed 200 spikes/s in the BFER (Young and Voigt 1982). In Fig. 4 the BFER is shown in black and is depicted as it appears in the response map of Fig. 2C, separated from other excitatory areas by inhibition in the *center* of the response map.

The second feature of typical type IV response maps is the central inhibitory area (CIA). This feature is present in all type IV units and, along with the BFER, is a defining characteristic of this response type. Operationally, the CIA is the inhibitory region centered near BF, the upper or lower frequency extents of which are delimited by excitatory areas (Fig. 2C, 20–40 dB attenuation), by areas of no response (Fig. 2D, 60–90 dB attenuation), or by bumps (increases in rate) in the inhibitory response that do not quite become excitatory (Fig. 2D, 20–50 dB attenuation). Two vertical lines mark the boundaries of the CIA at 30–40 dB above

inhibitory threshold for the units in Fig. 2. In the schematic in Fig. 4, the CIA is the shaded area at the *center* of the response map.

The CIA can be narrow and clearly defined, as shown in Fig. 2, or broad and poorly demarcated, like the units in Fig. 3. For some units (Figs. 2A and 3A), the inhibition gives way to excitation at very high sound levels (10 and 30 dB attenuation). Narrow CIAs resemble tuning curves of auditory nerve fibers in that they broaden at higher sound levels, but they differ from these curves in that low-frequency tails (Kiang and Moxon 1974) are usually not observed. The inhibition in the CIA is the strongest of any in the response map, as is evident from the flat bottoms on many rate profiles in Figs. 2 and 3, which indicate that discharge rate has been reduced to zero. Peristimulus time (PST) histograms in the CIA typically show a single onset

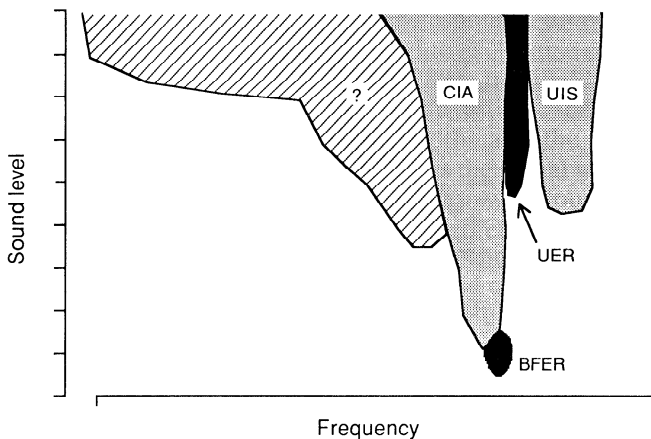


FIG. 4. Schematic of a type IV response map showing 4 features found in typical response areas. Excitatory areas are black; inhibitory areas are stippled. BFER, low-level excitatory region at BF; CIA, central inhibitory area; UER, excitatory region along the high-frequency (upper) edge of the CIA; UIS, upper inhibitory sideband. Regions at frequencies below the CIA (diagonal lines marked with a "?") are usually excitatory, but may be either excitatory or inhibitory.

spike followed by a reduction of rate to zero (Shofner and Young 1985) and are generally more complex, with offset spikes or afterdischarges, than PSTs of inhibitory responses in other frequency regions (Young and Brownell 1976).

The third feature of type IV response maps is an excitatory area (upper excitatory region, or UER) that lies along the high-frequency edge of the CIA (arrows above the response maps in Figs. 2 and 3). When present (42/49 units), the UER shifts slightly to higher frequencies with increases in level and defines a sharp high-frequency boundary for the CIA. Figures 2, A and C, and 3B show the UER clearly. In Fig. 2A the UER is continuous with the BFER, whereas in Fig. 2C the excitatory regions are separated by an inhibitory region. The response map in Fig. 2D shows regions of lessened inhibition along the high-frequency limit of the CIA that suggest a UER. The UER is shown in the schematic of Fig. 4 as an excitatory region like the one in the response map of Fig. 2C.

The fourth feature of type IV response maps is an upper inhibitory sideband (UIS). The UIS is most clearly seen when the high-frequency edge of the CIA is clear, as in Figs. 2, A and C, and 3B. The UIS varies in threshold and strength. A UIS was found in 44/47 response maps; two response maps, both constructed using rate-level curves, did not extend to high enough frequencies to allow the UIS to be seen. In five units, the UIS had a very high threshold or the CIA was irregular (generally nonmonotonic) so that the UER did not appear as a distinct feature, yet the UIS was clearly present in all five. For some units (Fig. 2C), the UIS appears to merge with the CIA at low sound levels, resulting in a low-threshold inhibitory area above the excitatory BF. The prevalence of the low-threshold inhibitory area above BF was assessed by selecting the subset of units that showed a clear UER (41 units) and looking for low-level inhibition in that frequency range. Low-threshold, above-BF inhibition is found in eight of these units. In Fig. 4, the UIS is depicted as having a clear threshold, as it appears in the response map of Fig. 2A. The low-threshold

inhibition above BF, which can merge with the UIS, is not shown in Fig. 4.

At higher levels for frequencies below the CIA, the response map consists of a variable mix of excitatory and inhibitory areas. The response of type IV units is usually excitatory at the highest sound levels for frequencies below BF, although exceptions occur (Fig. 3D). In Fig. 4, low-frequency regions are filled with a diagonal line pattern and marked with a "?" to indicate the variable patterns of excitation and inhibition found there.

The response maps shown in Figs. 2B and 3, A and C, illustrate the shape of response maps at the extremes of the BF range we studied. Low-BF response maps are shown in Figs. 2B and 3A. These are divided roughly into excitatory regions below and inhibitory regions above 3 kHz, but the inhibitory area encroaches on the excitatory area to create a nonmonotonic rate-level curve at BF. The highest BF response maps are exemplified by the one in Fig. 3C. This unit is classed as a 50.3-kHz type IV unit, as opposed to a lower BF unit with no BFER, because of its place in the tonotopic sequence of the DCN and because of its nonmonotonic rate-level curve at 50.3 kHz (Fig. 3C, *inset*). The apparent high threshold of the BFER of this unit is due to the sharp dropoff in stimulus energy above 30 kHz in our acoustic system. This unit has a large inhibitory area extending 30 kHz below BF, which is typical of DCN units tuned to very high frequencies. The rate-level function in the *inset* suggests that this inhibitory area extends to BF at higher levels, but this could not be tested with our acoustic system.

Units with both well defined and poorly defined CIAs are found in all layers of the nucleus (Table 1), with no apparent trend toward association of response type with depth. Because the number of units with poorly defined CIAs is small, this conclusion is still somewhat uncertain.

The response maps in Fig. 5 illustrate the behavior of units that fall into a gray area between the type IV and type III classes. Type III units give excitatory responses to BF tones at all levels and have upper or lower inhibitory sidebands, or both (Young 1984). Types III and IV are not sharply distinguished; there is a small number of units that form a continuum from one type to the other (Shofner and Young 1985). Figure 5A shows the response map of a type IV unit with a weaker CIA and larger excitatory regions than most type IV units. Figure 5B shows a unit that does not have a CIA in the sense of a region where rate decreases below spontaneous rate; nevertheless, this unit gives a nonmonotonic rate response at BF (*inset*) and has a region of rate decrease surrounding BF that resembles a CIA. The unit also shows upper and lower inhibitory sidebands. Units like the one in Fig. 5B are called type IV-T (for transitional) if their degree of nonmonotonicity at BF is such that the driven rate (i.e., rate minus spontaneous rate) increases to a maximum and then drops below 50% of that maximum within 35 dB of threshold. Type IV and type IV-T units are separated by requiring type IV units to show an inhibitory response (rate decrease from spontaneous rate) at some level for BF tones. The units in Fig. 5 straddle the type IV-type IV-T border. Type IV-T units are not included in the population studied in this paper.

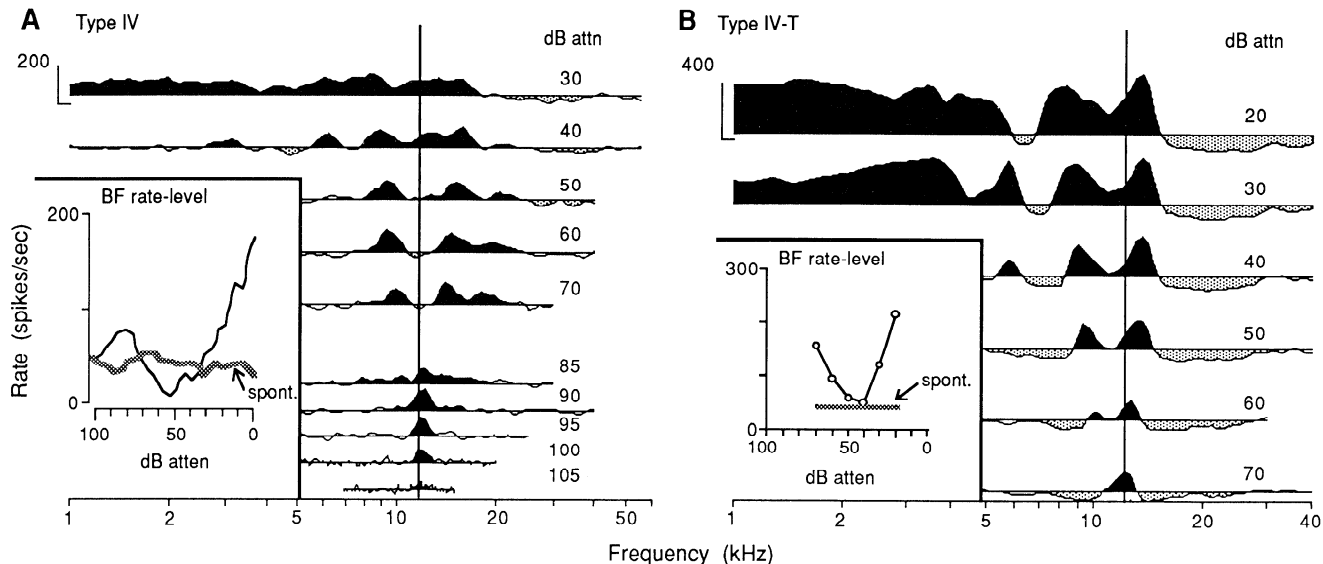


FIG. 5. Response maps of a type IV unit (*A*) and a type IV-T unit (*B*). BFs are indicated on response maps by vertical lines. CIAs for both units are weaker than are those for units shown in Figs. 2 and 3. *Insets*: rate-level curves at BF; rate-level curve in *A* has been smoothed. Actual BF rate-level data not available for unit in *B*, so rates plotted in the *insets* were read from the response map.

Tuning of central inhibition

The BF of the CIA can be defined as the frequency at which inhibition appears at the lowest level. Although this definition is straightforward, applying it in practice can be difficult. There is clearly an overlap of inhibitory and excitatory input in the vicinity of the CIA, because, when an anesthetic dose of pentobarbital sodium is given, the CIAs of type IV units are replaced by excitatory response areas (Evans and Nelson 1973a; Young and Brownell 1976). Given such overlap, the area where inhibition affects a unit need not correspond to the inhibitory area of the unit's response map, which is the region where the inhibitory input is stronger than the excitatory input. For the purposes of the bandwidth measures described in the next section and for the CIA BF determinations of this section, we define the inhibitory threshold as the point at which rate begins to decrease toward the CIA; this definition allows inhibitory thresholds to be within an excitatory area such as the BFER.

For response maps constructed from rate-level curves, the resolution of the data is good along the sound-level axis, so the inhibitory threshold is well defined in the vicinity of BF. In response maps constructed from frequency steps, however, the resolution of the data is good along the frequency axis, not the sound-level axis, so the inhibitory threshold is well defined on the sides of the CIA and is poorly defined in the vicinity of the CIA BF. The frequency at which the largest rate decrease is observed at low sound levels in response maps constructed from frequency steps could be used for the CIA BF by analogy to the method used to determine excitatory BF. This method probably does not yield a good estimate of CIA BF, especially in cases like those in Fig. 2, *B* and *C*, in which the CIA seems to be centered on the excitatory BF.

Figures 6 and 7 illustrate the behavior of inhibitory thresholds of two type IV units as determined from rate-

level data. Response maps constructed from rate-level curves (Figs. 6*A* and 7*A*) show the same features as those mapped with the use of frequency steps. The unit in Fig. 6 has low-level excitation (BFER) that shifts to higher frequencies with increases of intensity, forming the upper edge of the CIA (UER); this unit also has a well-defined CIA. The frequency range was not extended high enough to search for a UIS. The response map in Fig. 7 was extended to higher frequencies and has a UIS as well as low-threshold inhibition above BF.

Samples of the rate-level functions used to construct the response maps are shown in Figs. 6*B* and 7*B*. Inhibitory thresholds are marked at the top of each panel by a vertical line. Inhibitory threshold is most easily identified at frequencies near the excitatory BF, where the rate-level curves are nonmonotonic (Fig. 6*B*, *h* and *i*; Fig. 7*B*, *f-h*), and is taken as the point at which rate begins to decrease toward the CIA. At frequencies away from BF, rate-level curves are monotonically inhibitory, and inhibition is marked at the point at which driven rate decreases consistently below spontaneous rate. Immediately above the BF region in Fig. 6*B*, *j-l*, the rate-level curves become excitatory as the stimulus passes through the UER, and inhibitory thresholds do not exist.

Inhibitory thresholds are plotted on the response maps in Figs. 6 and 7 as circles connected by lines. Away from excitatory regions, the inhibitory thresholds lie close to the edge of the response map inhibitory regions; however, the inhibitory thresholds clearly lie within the BFER for frequencies near BF. The CIA in Fig. 6*A* is tuned below the excitatory BF of the type IV unit (at ~6.69 kHz, *f*). The inhibitory area in Fig. 7*A* has bimodal tuning, with one minimum at 12.4 kHz (*e*) and another at 15.6 kHz (*i*). Inspection of the inhibitory region shows a line of decreased inhibition connecting the BFER to the UER; this line separates the CIA from the UIS and other above-BF inhibition. It seems rea-

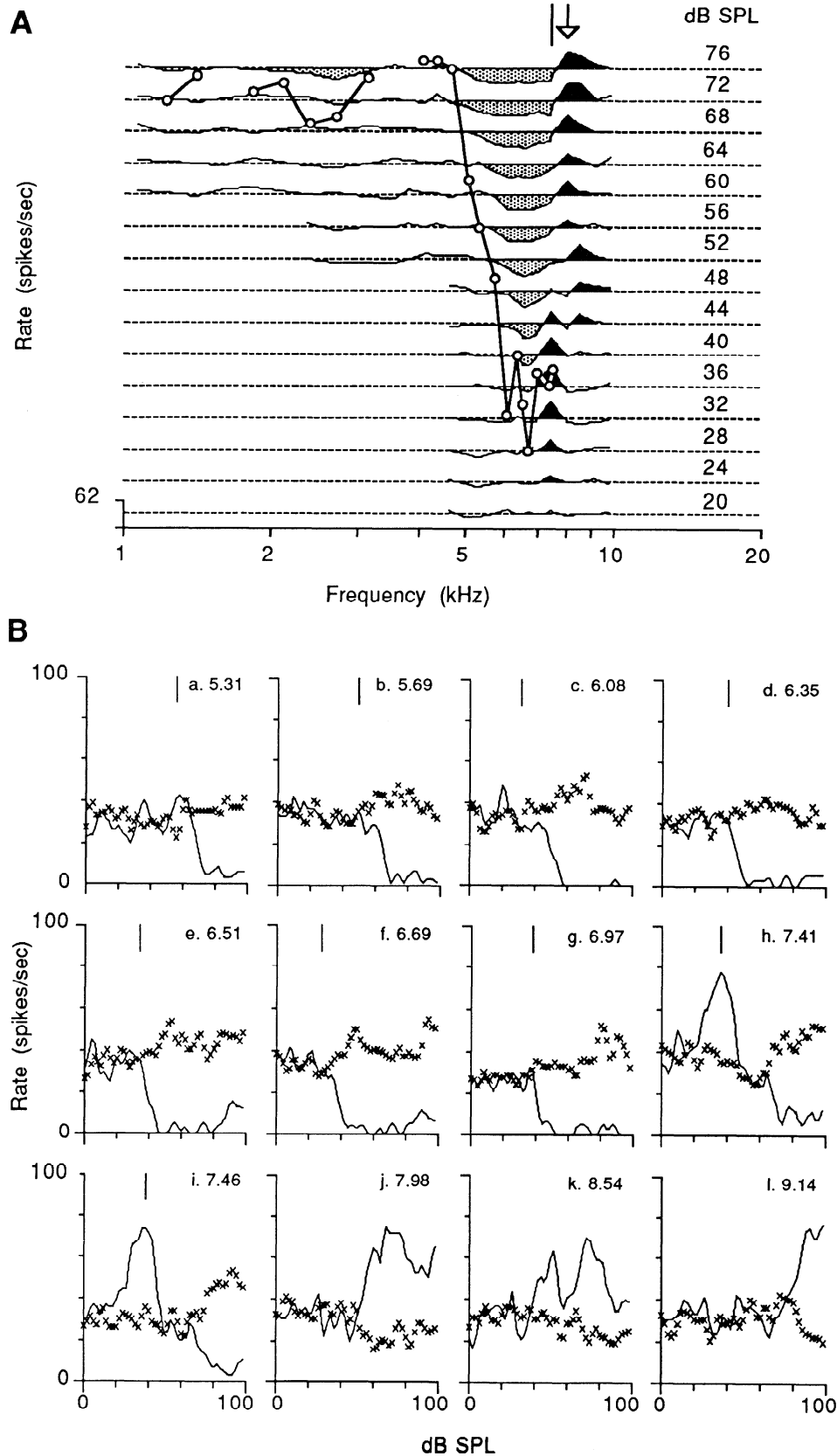


FIG. 6. *A*: response map constructed from rate-level plots. Same conventions as in Figs. 2 and 3, except rate scale is at *bottom left* and sound level is displayed in dB SPL. *B*: rate-level curves at frequencies in the central part of the response map. Tone frequency is given at the *top* of each graph. Solid lines are driven rates, \times s are spontaneous rates (i.e. spontaneous rate during the 190 ms immediately before each tone burst). Inhibitory thresholds are marked with vertical lines *above* each rate-level curve. BF is panel *h*; CIA BF is panel *f*. On the response map, inhibitory thresholds are marked with circles and connected with heavy lines. BF 7.41 kHz, spont rate 34 spikes/s, not localized.

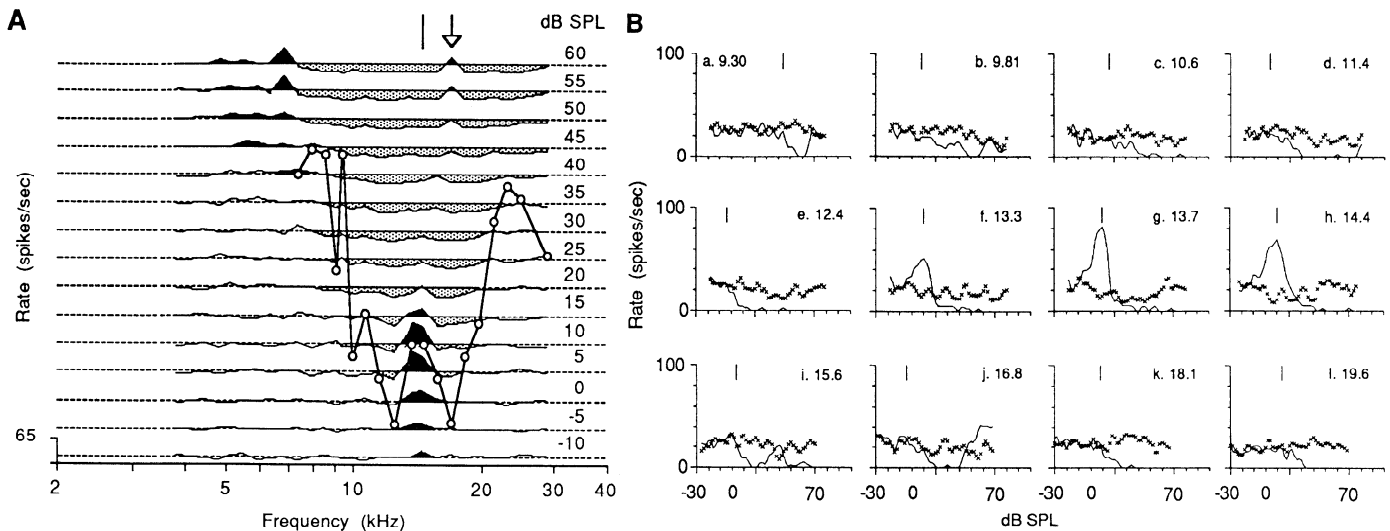


FIG. 7. *A*: response map constructed from rate-level plots. *B*: rate-level curves. Same conventions as Fig. 6. Excitatory BF is panel *g*; CIA BF is panel *e*. BF 13.7 kHz, spont rate 20 spikes/s, not localized.

sonable to assign the lower inhibitory BF (12.4 kHz) to the CIA, making this unit's CIA BF below its excitatory BF (13.7 kHz, *f*). The upper inhibitory BF (16.8 kHz, *i*), then, is the BF of the combination of the UIS and low-level, above-BF inhibitory area; this is the lowest threshold for above-BF inhibition in our data sample.

In Fig. 8, the ratio of CIA BF to excitatory BF is plotted against excitatory BF for units for which response maps were constructed with the use of rate-level curves (\square). The line shows where the two BFs are equal. Most (8/11) of the symbols fall below the line, indicating that the CIA tends to be tuned below the excitatory BF of the type IV unit. For comparison, the same ratio is plotted for type IV response maps determined with frequency steps (\blacksquare). In these cases, the CIA BF was determined in the following indirect fashion. For the response maps generated with the use of rate-

level curves that have well-defined CIAs, the inhibitory BF is, on average, 0.62 of the way (on a log scale) between the lower and upper edges of the 40-dB bandwidth of the unit (SD 0.085). This calculation was applied to response maps generated with the use of frequency steps with well-defined CIAs only. The CIA BF defined in this way also seems to be slightly below the excitatory BF (Fig. 8, \blacksquare) and seems to scatter over about the same range as the CIA BF defined from rate-level curves (the medians of the CIA BF/excitatory BF ratios are 0.96 for the frequency-step data and 0.89 for the rate-level data).

Bandwidth of central inhibition

For most type IV units (44/49), the CIA is demarcated clearly enough that it is possible to measure its bandwidth. For comparison with previous work on bandwidths of DCN type II units (Young and Voigt 1982), we computed an estimate of the CIA bandwidth at 40 dB above the inhibitory threshold. Because the resolution of sound level in response maps is generally 5 or 10 dB near threshold, the bandwidth is measured at 30 dB above the lowest sound level showing inhibition. This procedure results in a measure that is 35–40 or 30–40 dB above the actual inhibitory threshold, depending on the resolution of the response map measurements. Therefore the results based on this definition are slightly conservative estimates of the 40-dB bandwidth.

Bandwidths are measured from edge to edge of the inhibition. When the CIA is bordered by an excitatory area, as is often the case along the high-frequency edge (bordered by a UER), the inhibitory edge is taken as the peak of excitation, i.e., where rate begins to decrease toward the inhibitory area (e.g., Fig. 2, *A* and *C*). If the peak is broad and flat topped, the knee of the excitation is taken as the edge. The same criteria are applied to the low-frequency edge. Often, however, the inhibition does not have an excitatory border at one or both edges. In these cases, the return to spontaneous rate is marked as the inhibitory edge (e.g., Fig. 2*B*). The

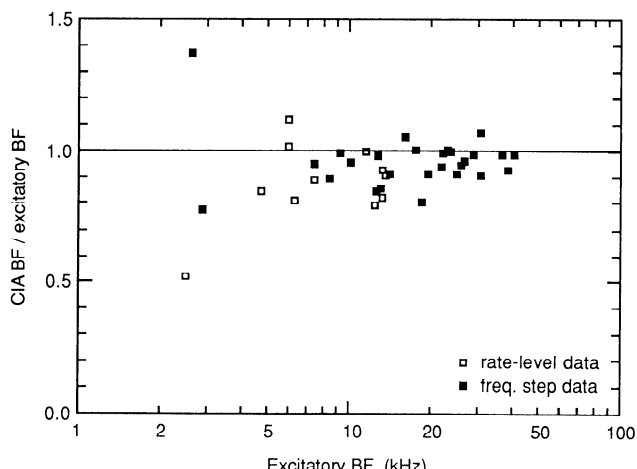


FIG. 8. Plot of the ratio CIA BF/excitatory BF against excitatory BF for 11 units with response maps that were constructed from rate-level curves (\square) and 27 units with response maps that were constructed from frequency steps (\blacksquare). These 27 units are the same units with narrow, well-defined CIAs for which data are plotted with filled squares in Figs. 9 and 10. Methods of defining CIA BF described in text. Line indicates equal BFs.

response maps in Fig. 2 have been marked with pairs of vertical lines to indicate the edges of the CIA and the sound levels at which measurements were made. A plot of estimated 40-dB bandwidth versus excitatory BF is shown in Fig. 9; CIA BF is not used on the abscissa in Fig. 9 because there is no reliable way to determine CIA BF for the units with poorly defined CIAs. From Fig. 8, the difference between CIA and excitatory BF should be small. Data from 35 units judged to have clearly defined CIA edges (e.g., Figs. 2, 5A, and 11–13) are plotted with squares, and data from 9 units with indistinct CIA edges (e.g., Fig. 3) are plotted with circles. The line separates units of the two categories, except for one unit. The units falling below the line most consistently display the features of type IV response maps summarized in Fig. 4. For this reason, the units falling below the line are used below to quantify features of the CIA and to interpret the responses of type IV units to bandlimited noise.

Quality factors (Q_{40}) for CIAs are computed by dividing the estimates of CIA BFs by the estimates of 40-dB bandwidths. The CIA BFs defined in the previous section were used, but the results in Fig. 10 depend neither on the definition of CIA BF nor on whether excitatory BF or CIA BF is used. Q_{40} values for CIAs are plotted in Fig. 10 along with similar values for type II units' excitatory areas. Type II units are chosen for the comparison in Fig. 10 because of the evidence suggesting that type II units are the inhibitory interneurons responsible for producing type IV units' CIAs (Voigt and Young 1980, 1990). The line separates most of the type IV CIAs (29/35, or 83%) from the type II units (45/50, or 90%). Q_{40} s for CIAs fall below those for type II units, indicating that type IV CIAs are wider, on average, than type II unit tuning curves. Some caution must be exercised because the range of BFs in the sample of type II units does not fully overlap that of the type IV units. Nevertheless, over the decade range of BF overlap, these data suggest that, if type IV CIAs result from inhibitory input from type II units, then a CIA represents the convergent activity of

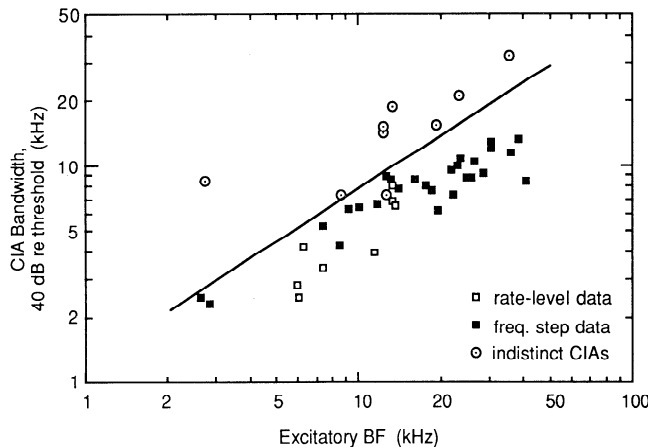


FIG. 9. CIA bandwidth ~ 40 dB above inhibitory threshold for 44 type IV units plotted against the units' excitatory BFs. Squares show data from units with clearly defined CIA boundaries; circles show data from units with poorly defined CIAs (8 units from this study, 1 from Voigt and Young 1990). Filled squares are from response maps determined with frequency steps (27 units from this study), and open squares are from response maps determined from rate-level curves (8 units from Voigt and Young 1990).

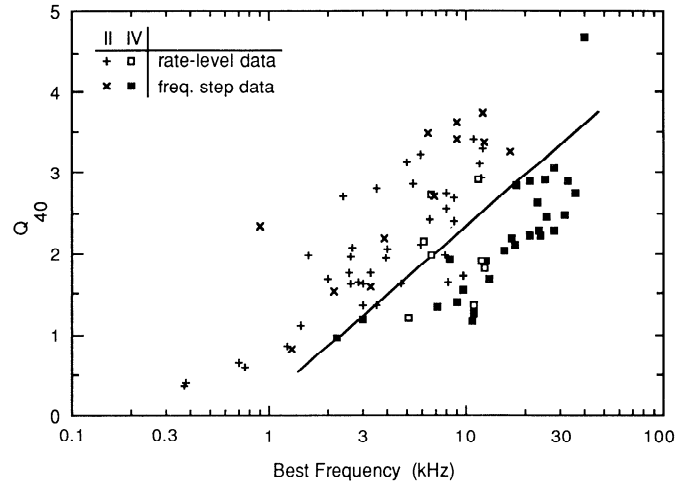


FIG. 10. Q_{40} vs. BF for type II units' excitatory areas (+ and \times) and type IV units' CIAs (\square , ■). Thirty-eight type II units from Young and Voigt (1982) are indicated by +; \times show 12 type II units from this study. Square symbols for type IV CIAs defined as in Fig. 9. Line is plotted to demonstrate differences in Q_{40} of the 2 unit types.

more than one type II unit. The ratio in Q_{40} values between the unit types (type II/type IV) covers a range from 1 to 3, indicating that a minimum of one to three type II units with nonoverlapping response maps converge to form the CIA of a type IV unit.

Response to notch noise stimuli

Figure 11 shows the response map of a type IV unit and its responses to broadband noise and to notch noise stimuli. Figure 11A shows the acoustic calibration for the experiment in which the data in the rest of the figure were obtained; the notch noise spectra (like those in Fig. 1) are modified by this calibration, which produces fluctuations over a 15-dB range across the frequency spectra of the noise signals. Figure 11B shows the unit's response map. Over a range of levels from -40 to -70 dB, the responses of this unit to tones are predominantly inhibitory. One might assume that a unit's response map is a predictor of its responses to noise in that the responses to noise could be predicted by computing a weighted sum of its responses to tones at various frequencies, where the weighting factors are the energies in the noise in narrow bands centered on the tone frequencies. Such a model predicts that the unit in Fig. 11 should give inhibitory responses to BBN (or any noise band centered on the unit's BF) over a 30- to 40-dB range of levels that begins ~ 10 dB above threshold. As has been shown previously (Young 1984; Young and Brownell 1976), this expectation is not realized in type IV units. Figure 11D shows rate-level functions from this unit for BF tones (BF) and BBN. The predicted inhibitory response is not seen in the noise rate-level function, which is strictly excitatory.

The responses of type IV units to notch noise stimuli provide another way of looking at the problem of the relationship between response maps and responses to complex stimuli. Figure 11E shows rate-level functions for responses of this unit to notch noise stimuli with four notch widths (see key). Figure 12D shows a more detailed example for

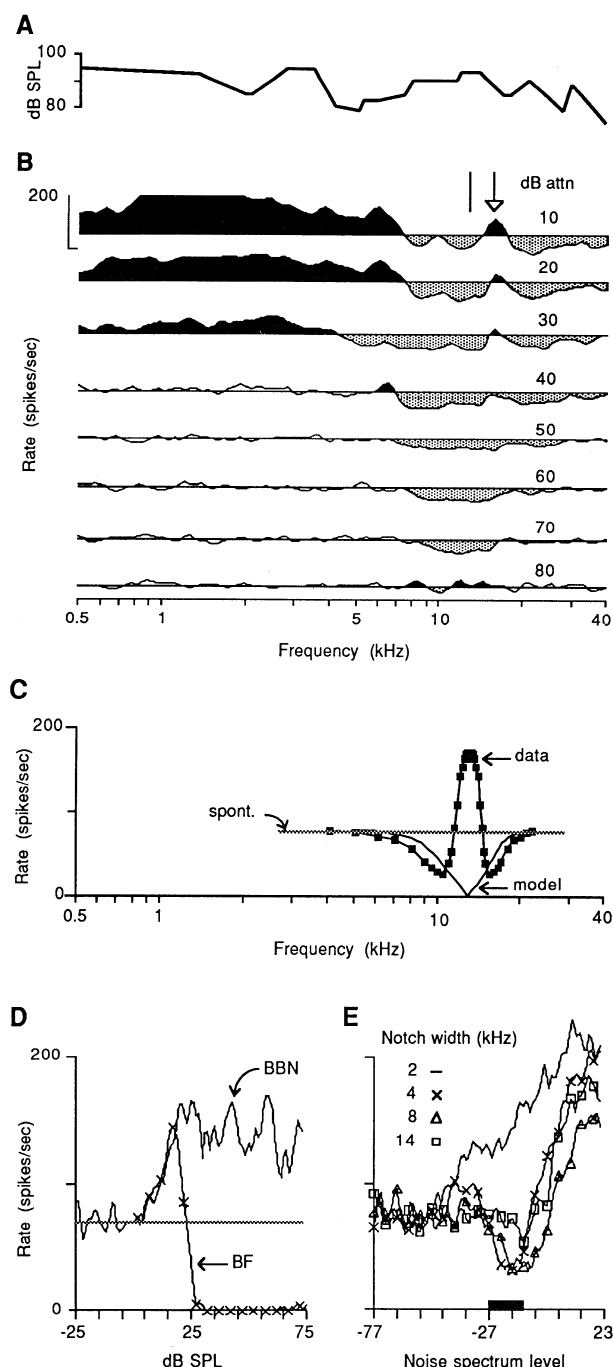


FIG. 11. A: acoustic calibration for the experiment in which data in parts B-E were obtained; shows SPL at 0 dB attenuation at various frequencies. Frequency scale is same as that of the response map in B. B: response map of a type IV unit in the same format as in Figs. 2, 3, and 5. C: rate vs. notch noise cutoff frequency for this unit ("data," filled squares) and for predictions made from the response map ("model," line with no symbol). Average spontaneous rate shown by stippled line. Rate for each notch width is plotted twice, at the upper and lower cutoff frequencies of the stopband. Rates are averaged over noise spectrum levels marked with heavy bar on rate-level curves in E. D: rate-level curves for BF tones (BF) and broadband noise (BBN). Abscissa is dB SPL for the BF tone only; noise curve is shifted into alignment with BF tone curve at threshold. Spontaneous rate is shown by stippled line. E: rate-level curves for responses to notch noises of 4 notch widths, given in the key. Abscissa is spectrum level of passband with acoustic calibration value at unit's BF. Heavy bar shows range of levels over which rate was averaged to compute data in part C. BF 13.1 kHz, spont rate 76.4 spikes/s, not localized.

another type IV unit, whose response map and acoustic calibration are also shown, in the same format as in Fig. 11. At the narrowest notch widths (2 kHz in Fig. 11, 1 kHz in Fig. 12), one sees strictly excitatory responses similar to those generated by BBN. At wider notch widths (4 and 8 kHz in Fig. 11, 2 and 5 kHz in Fig. 12), a clear inhibitory response develops at intensities 20–30 dB above the BBN excitatory threshold (heavy bar on the abscissas of both figures). The inhibition disappears at wide notch widths

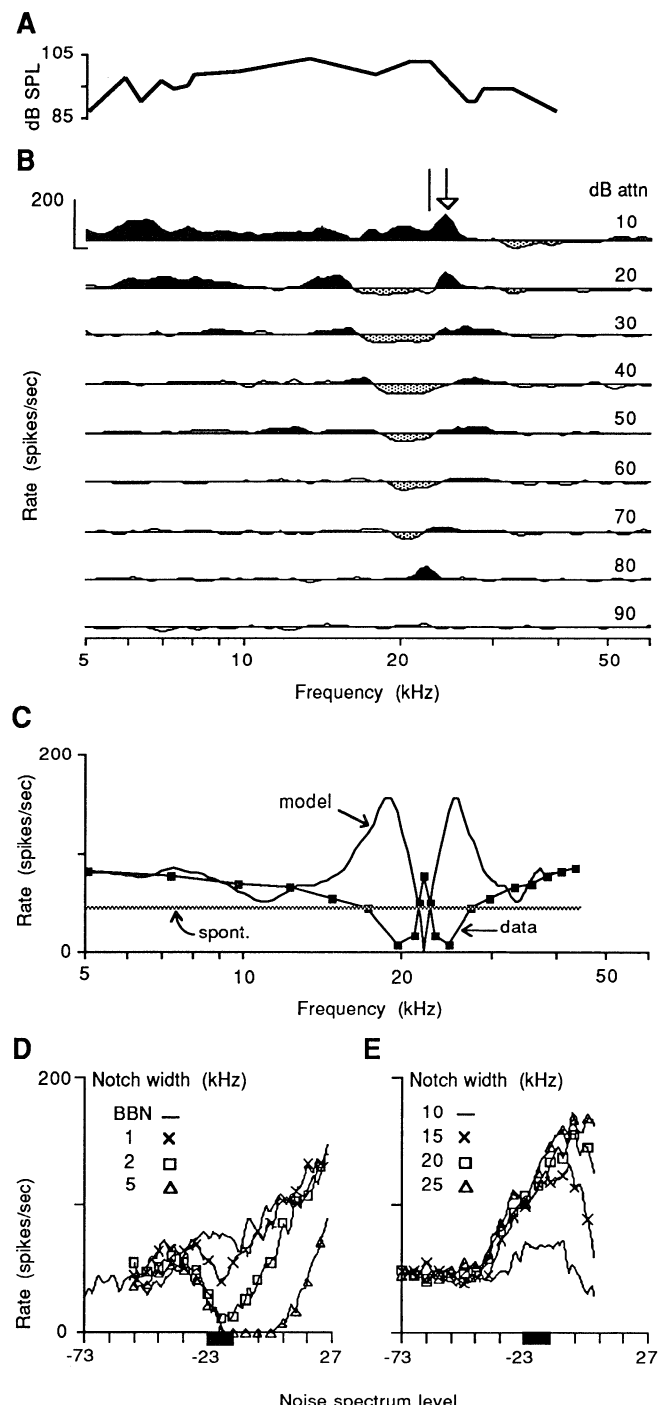


FIG. 12. Same format as in Fig. 11, except that D shows rate-level functions for BBN and notch noise and not for BF tones. BF 22.3 kHz, spont rate 45.6 spikes/s, not localized.

(14 kHz in Fig. 11, 10 kHz in Fig. 12), and the responses at the widest notch widths (15, 20, and 25 kHz in Fig. 12) are similar to the response to BBN, except for an increase in threshold; these wide-notch-width responses probably reflect, at least in part, a response to the BBN floor of the notch, as may the responses to narrower notch widths at high sound levels.

The relationship between notch noise responses and the response map can be studied by plotting discharge rate in response to notch noise versus notch width on a frequency axis comparable with the response map's axis. Rates in response to notch noise were computed by averaging rate-level functions over a 10- to 15-dB range selected to capture the inhibitory responses. The ranges used for the units in Figs. 11 and 12 are marked by the heavy bars on the abscissas of the notch noise rate-level functions (Figs. 11E and 12D). The levels used for these averages are low enough that there should be little response to the noise floor of the notches. The resulting average rates are plotted as functions of the cutoff frequencies of the notch noise in Figs. 11C and 12C; they are the plots marked "data" and are called *rate-versus-cutoff-frequency functions* below. Note that the frequency scales in Figs. 11C and 12C are aligned with the frequency scales of the response maps. The rate-versus-cutoff-frequency functions have mirror-image symmetry (except for the logarithmic frequency axis) around their centers (equal to the units' BFs) because average rate for each notch width is plotted twice, once at the cutoff frequency of the lower edge of the notch and once at the cutoff frequency of the upper edge of the notch. The stippled horizontal line represents spontaneous rate, so that rates below this line represent net inhibition.

The rate-versus-cutoff-frequency functions in Figs. 11C and 12C are typical of our data in that the average rate has a valley-peak-valley shape centered on the narrowest notch widths. There is a rate maximum at the narrowest notch widths (corresponding to the response to BBN); the rate declines to become inhibitory at wider notch widths and then returns to spontaneous levels (Fig. 11) or to a value above spontaneous levels (Fig. 12), reflecting a response to the noise floor of the notch.

The disagreement between the response map and the BBN responses discussed earlier also appears when comparing response maps and rate-versus-cutoff-frequency functions. Essentially, the rate-versus-cutoff-frequency functions predict an excitatory response area in the vicinity of BF. To see this, note that response rate increases as energy is added to the notch noise in a narrow-frequency band around the BF; that is, rate increases from the bottom of the valley in the rate-versus-cutoff-frequency function to its excitatory peak at zero notch width. Therefore this frequency range should contain an excitatory response area in the response map. In fact, most of the response map in the frequency range of the predicted excitatory area is taken up by the CIA.

Twelve type IV units were studied with notch noise stimuli. Eleven of these had narrow well-defined CIAs, and the results from those units are described here. Their BFs range from 8.66 to 39.7 kHz. The plots in Figs. 11C and 12C are typical of the results for all 11 units in that the rate-versus-

cutoff-frequency functions have a valley-peak-valley shape near BF and in that the excitatory area near BF that is predicted by the rate-versus-cutoff-frequency functions does not appear in the response map. However, it is interesting to note that the bandwidth of the predicted excitatory area (i.e., the frequency range between the bottoms of the 2 valleys in the rate-versus-cutoff-frequency functions) corresponds roughly to the bandwidth of the BFER of the response map. The bandwidth of the predicted excitatory area is between 1 and 1.21 times the bandwidth of the BFER at its widest point in nine cases and is narrower than the BFER in the other two.

The lack of a clear relationship between response maps and rate-versus-cutoff-frequency functions can be demonstrated in a more quantitative fashion by the use of the response map to predict the rate-versus-cutoff-frequency functions with a quasilinear energy summation model. These calculations are done by summing rates in the response map over the frequency ranges within the passbands and the stopband of the notch noise. The sound level used for the passband is chosen to be the same number of decibels above the BF tone threshold as the center of the range of levels used to compute rate-versus-cutoff-frequency functions is above BBN threshold (in terms of spectrum

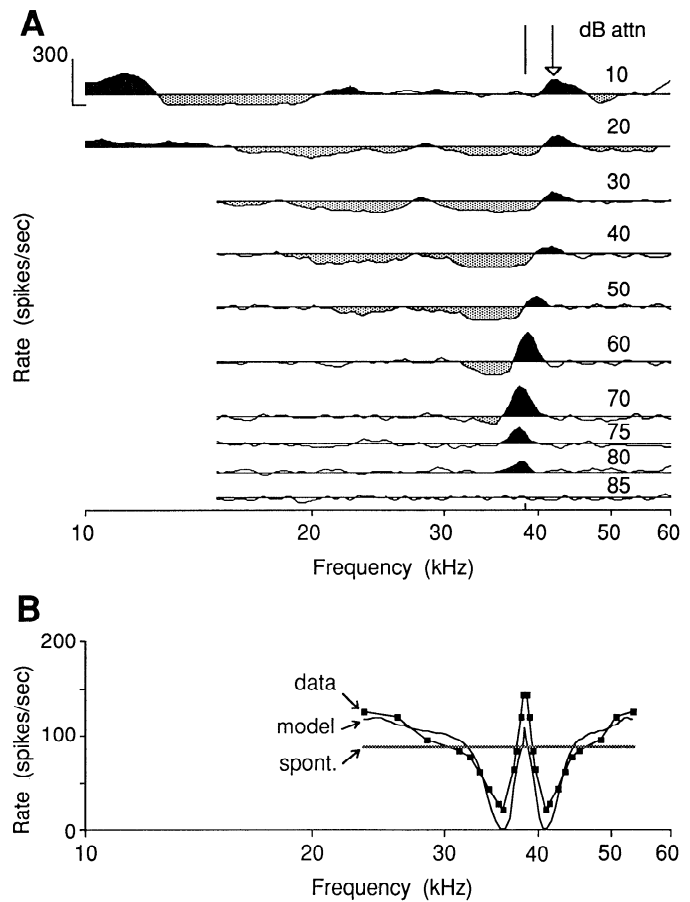


FIG. 13. Response map (A) and rate-vs.-cutoff-frequency functions (B) in the same format as Figs. 11 and 12. This was the only unit for which predicted rate-vs.-cutoff-frequency function (model) matched its measured profile (data). BF 38.5 kHz, spont rate 73.4 spikes/s, pyramidal cell layer.

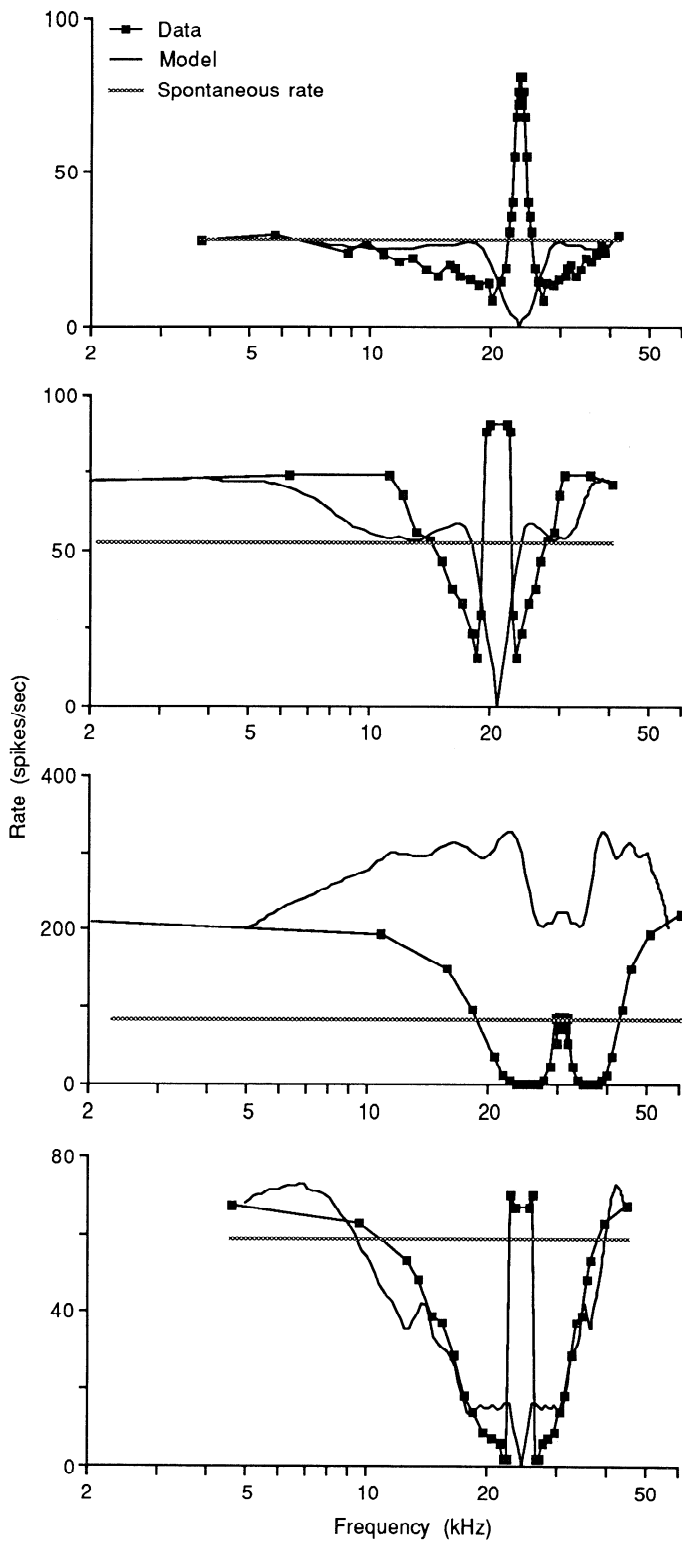


FIG. 14. Comparison of rate-vs.-cutoff-frequency functions from 4 additional units (data) with the predictions from their response maps (model). Spontaneous rates shown by stippled lines.

level). The sound level for the stopband is set 30 dB below that used for the passband. The logarithmic frequency scale of the response map is accounted for by weighting each rate by the frequency step (in hertz) between the rate and the next point in the response map.

The computation can be described by the equation below, which expresses the predicted rate-versus-cutoff-frequency-function $p(w_n)$ in terms of notch bandwidth w_n

$$p(w_n) = \sum_{f_k \in PB(w_n)} r(f_k, L_{PB})(f_{k+1} - f_k) + \sum_{f_k \in SB(w_n)} r(f_k, L_{SB})(f_{k+1} - f_k) \quad (1)$$

where $r(f, L)$ is the response map, expressed as the response rate at frequency f and sound level L minus spontaneous rate; the $\{f_k, k = 1, \dots, N\}$ are the N frequencies at which response map data were taken; $PB(w_n)$ is the set of response map frequencies within the passband of a notch noise with notch width w_n ; $SB(w_n)$ is the set of response map frequencies within the stopband of the same noise; L_{PB} is the response map attenuation corresponding to the passband level of the notch noise as defined above; and L_{SB} is the response map attenuation corresponding to the stopband level of the noise ($L_{SB} = L_{PB} - 30$).

The lines plotted without symbols (marked "model") in Figs. 11C and 12C show model rate-versus-cutoff-frequency functions computed from the response maps [i.e., $p(w_n)$]. The model functions are aligned vertically with the data functions at very low frequencies and are scaled so that their peak negative value just reaches 0. These alignment and scaling operations are done so that the shapes of the curves can be compared without worrying about the correct vertical scale for the model function (this arbitrary scaling is necessary because no scaling was done in Eq. 1 to compensate for the effects of the frequency difference factors). Figures 11C and 12C show dramatically the difference between predicted and measured responses in that the predicted response to narrow notches is strong inhibition of the unit, in contrast to the actual excitatory response.

Figure 13 is organized similarly to Figs. 11 and 12, except that rate-level functions are not shown. The unit in Fig. 13 is the only unit of the 11 studied in which the predicted rate-versus-cutoff-frequency function has the same shape as the data. In this case, the predicted rate-versus-cutoff-frequency function has a maximum at BF because the firing rate in the UER is high, the highest among the units in our sample.

Figure 14 shows a comparison of the actual and predicted rate-versus-cutoff-frequency functions for four additional units. Each plot shows the actual (■) and predicted (—) functions for one unit. All four plots are similar to those in Figs. 11 and 12 and are typical of 10/11 units for which this analysis was carried out in that the predicted and actual functions are the inverse of each other at narrow notch widths. In particular, note that the predicted functions have a rate minimum at narrow notch widths, whereas the actual functions have a peak in every case.

DISCUSSION

Response maps

Previous descriptions of type IV response maps (Evans and Nelson 1973a; Young and Brownell 1976) have emphasized their generally inhibitory nature and their complexity. Our results show that type IV units consistently receive an inhibitory input that forms their CIAs and that

the response maps have other consistent organizational features. Construction of response maps with the use of sampling intervals of 0.02–0.05 octaves along the frequency axis has permitted the identification of sharp boundaries between response map features. Plotting the results as discharge rate, rather than simply as net excitation or inhibition, has revealed features within excitatory and inhibitory regions. Finally, we sampled type IV units with BFs spanning nearly the entire range of cat hearing and show that type IV units exhibit the same response map features across the entire frequency range. Earlier studies have reported type IV units with BFs generally <15 kHz (Evans and Nelson 1973a,b; Young and Brownell 1976).

Response maps constructed with the use of pure tones of varying frequency and intensity provide an overview of all inputs to type IV cells that are activated by this stimulus. These results reveal that most type IV units show two inhibitory and two excitatory regions. We will argue below that the two excitatory regions reflect the same source of input, whereas the CIA and UIS appear to result from different inhibitory inputs. Type IV units having these well-defined response map features are found in both pyramidal cell and deep layers of the nucleus (Table 1), which is a curious finding, given the different cellular organization of these regions of the nucleus (Blackstad et al. 1984; Lorente de Nò 1981; Mugnaini 1985; Wouterlood and Mugnaini 1984). Most likely, the similarity of superficial and deep type IV unit responses reflects a similarity in synaptic organization of the pyramidal and giant cells with regard to type II inhibitory input (Osen et al. 1990; Saint Marie et al. 1991) and a lack of strong activation, in our experiments, of the circuitry in the superficial DCN, which contacts only pyramidal cells.

Response map features reflect the dominant inputs in a particular frequency region and do not reveal underlying excitatory and inhibitory inputs. The possibility that important inputs to type IV cells are masked by the use of this technique is suggested by experiments of Shofner and Young (1987). Lidocaine injections into the AVCN in regions containing fibers that connect the AVCN and DCN sometimes result in an increase in UER amplitude, indicating that an intranuclear inhibitory input is present in the frequency range dominated by this excitatory response feature.

Excitatory inputs

All type IV units have a BFER. Of course, this statement is part of the definition of type IV units (Evans and Nelson 1973a; Young and Brownell 1976); initially, a separate response type, type V, was reserved for units with CIAs but no BFERs in their response maps. In fact, very few type V units are actually seen, and there is always doubt about whether a small or a weak BFER (as in Fig. 3D) has been missed. The BFER is of narrow bandwidth and seems to represent the tip of the tuning curve of the principal excitatory drive of the unit. This conclusion follows from the notch noise responses because omission of stimulus energy at frequencies within the BFER by widening a noise notch centered on BF always results in a decrease in discharge rate

(Figs. 11–14). In addition, when an anesthetic dose of pentobarbital sodium is administered, the CIA disappears, revealing an excitatory region with a typical auditory tuning curve that has the same BF as the original BFER (Evans and Nelson 1973a; Young and Brownell 1976).

At levels greater than ~25 dB above BF threshold, the most consistently appearing excitatory area is the UER. The UER is separated from the BFER in the response maps of those units in which the center frequency of the CIA is located over the excitatory BF. The continuity of the BFER and UER is apparent in many units, especially those in which the CIA is displaced toward lower frequencies or is weak. For example, the CIAs of the type IV and type IV-T units shown in Fig. 5 are weak, appearing as a decrease in excitation within the excitatory surround. The presence of the UER has been reported previously (Evans and Nelson 1973a,b; Young and Brownell 1976) but has not been identified as a consistent feature of type IV response maps.

Figure 15 shows a schematic model that accounts for the major features of type IV response maps. There is an excitatory input (shaded areas) that is partly occluded by the tuning curves of two strong inhibitory inputs (labeled type II units) that produce the CIA. These inputs are assumed to be strong enough to overwhelm the excitatory input whenever they are activated. An additional weak inhibitory input is shown for the UIS. The BFER and UER are produced by the arrangement of the strong inhibitory inputs, the BFs of which are slightly below that of the excitatory input and the thresholds of which are several decibels above that of the excitatory input. As a result, the tip of the excitatory input's tuning curve extends below the CIA to form the BFER; the higher-frequency edge of the excitatory input's tuning curve forms the UER. Evidence supporting these features of the inhibitory input is discussed below. The model can account qualitatively for variations in the strength of the UER and the continuity of the UER and BFER by changing the tuning of the strong inhibitory inputs. Clearly, as the

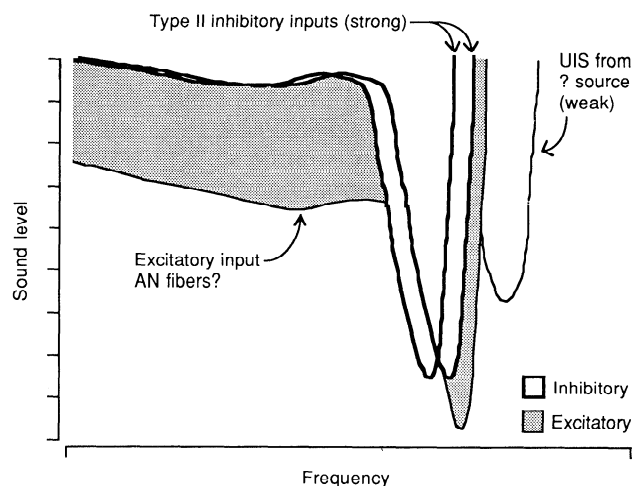


FIG. 15. Superposition of tuning curves of 3 neural elements to form a response map with the most commonly observed features of type IV units. Shaded region is the tuning curve of excitatory input from an auditory nerve fiber or other similarly tuned element. Excitatory tuning curves of 2 inhibitory interneurons, most likely type II units, are shown as unshaded areas bounded by heavy lines. Finally, there is a weak input from an unidentified source forming the upper inhibitory sideband.

inhibitory inputs' BFs move to higher frequencies, the UER will weaken and disappear as an excitatory area.

The most likely source of the excitatory input is the auditory nerve. Auditory nerve fibers are distributed in deep layers of the nucleus, with the external boundary of their domain in the pyramidal cell layer (Cohen et al. 1972; Jones and Casseday 1979; Osen 1970; Smith and Rhode 1985). They are good candidates as the source of the BFER and UER because they probably innervate both pyramidal and giant cells (Kane 1974; Smith and Rhode 1985), which are the cell types associated with type IV responses. Current source-density analysis along the vertical axis of pyramidal cells is consistent with a short-latency excitatory input from auditory nerve fibers onto the basal dendrites of pyramidal cells (Manis and Brownell 1983). A second possible source of excitatory input to DCN principal cells is posteroventral CN (PVCN) stellate cells (Oertel et al. 1990; Smith and Rhode 1989), the axons of which send collaterals to the DCN and can have terminals with excitatory morphology. Whether these axons contact DCN principal cells is not known. The excitatory tuning curve in Fig. 15 is modeled on the tuning curves of auditory nerve fibers with BFs >3 kHz (Kiang and Moxon 1974); in particular, at low frequencies the tuning curve has a tail that is ~50 dB above its BF threshold.

An unlikely source for the primary acoustically driven excitatory input to type IV units is the cochlear nucleus granule cell, the axon of which makes excitatory contacts on the apical dendrites of pyramidal cells in the molecular layer (Hirsch and Oertel 1988; Manis 1989; Mugnaini et al. 1980a). This system appears to lack requisite frequency specificity, because electrical activity can propagate along granule cell axons for long distances orthogonal to the DCN's isofrequency laminae (Manis 1989; Mugnaini et al. 1980b).

CIAs

A variety of evidence suggests that strong inhibitory input to type IV units is provided by DCN type II units and that this input accounts for the CIA. This evidence includes the fact that the responses of type II units to a variety of stimuli are reciprocal to those of type IV units (Young and Brownell 1976; Young and Voigt 1981) and that cross-correlograms of the spike trains of simultaneously isolated type II-type IV unit pairs show the features expected of a monosynaptic, inhibitory synapse (Voigt and Young 1980, 1990). The thresholds of type II units are elevated relative to those of type IV units by about the amount necessary to account for the BFER (Voigt and Young 1980; Young and Brownell 1976; Young and Voigt 1981). This fact is the justification for the elevated thresholds of the strong inhibitory inputs in Fig. 15. Comparison of Q_{40} measurements for CIAs and type II units (Fig. 10) suggests that between one and three type II units, aligned edge to edge along the tonotopic axis, would be needed to account for the CIA. Convergence of two type II units is assumed in the schematic diagram in Fig. 15. The actual number of type II units converging on a type IV unit is unknown, but estimates from cross-correlation measurements indicate that as many as 40

type II units, which could have overlapping BFs, may converge on one type IV unit (Voigt and Young 1990).

The fact that the bandwidths of CIAs are larger than those of type II units requires that some of the type II units converging on a type IV unit have BFs different from that of the type IV unit. Direct estimates of CIA BFs suggest that type II BFs are below that of the type IV unit on which they terminate (Fig. 8). Results from cross-correlation studies are consistent with this conclusion (Voigt and Young 1990). This organization is pictured in Fig. 15. There the type II BFs are below the BF of the excitatory input, which equals the excitatory BF of the type IV unit. The alignment of type II and type IV BFs is important in considering hypotheses about the responses of type IV units to complex stimuli (discussed below).

Type II units have tails like those of auditory nerve fibers, but they are at a much higher sound level, generally 70–90 dB above threshold (Young and Voigt, 1982). This fact is included in Fig. 15, in which the tails of the strong inhibitory input are well above the tail of the excitatory input. The result is that the tail of the excitatory input appears at frequencies below BF as an excitatory area in the type IV response map. This feature is frequently observed but is not always present (e.g., Figures 3D, 6A, and 13A). The model in Fig. 15 cannot be easily modified to account for the lack of a low-frequency excitatory area in some type IV response maps without adding more inputs.

The model also appears to have problems at very high sound levels, where type IV response maps frequently show a loss of the CIA (e.g., Figs. 2A, 3A, 5A, 12A, and 13A). However, the weakening of inhibition at high levels may be a result of the nonmonotonic responses of type II units to tones (Young and Voigt 1982); substantial reduction in type II discharge rate usually occurs at high stimulus levels. The fact that the effects of the tails of type II units are not seen as an inhibitory area in type IV response maps at high levels and low frequencies requires further study, because few type IV response maps are carried to high enough sound levels to see this inhibitory area.

An important assumption for our determination of inhibitory thresholds and bandwidths in type IV response maps is that the inhibitory threshold corresponds to the sound level at which rate begins to decrease toward the CIA. This method of assignment of inhibitory thresholds is based on studies of simultaneously isolated pairs of units consisting of a type IV and a type II unit (Young and Voigt 1981). When the cross-correlogram of the spike trains of the two units shows features that are consistent with a monosynaptic inhibitory connection from the type II to the type IV unit, the excitatory threshold of the type II unit occurs near the turnover point in the type IV unit's rate response.

UISs

The UIS is present in most type IV units, but can appear as 1) a small, high-threshold area (Fig. 3B); 2) a well-defined, bowl-shaped region of moderate threshold (Fig. 2A); or 3) an area extending along the UER to frequencies just above the excitatory BF at the same low threshold (Fig. 7). In the first two situations, the UIS resembles a single class of

inputs in much the same way as does the CIA. The third situation is more complex and may indicate convergence of multiple kinds of above-BF inhibitory inputs onto type IV cells. Evidence for a low-threshold above-BF inhibitory input, which may in part overlie the UER at higher levels, comes from the previously mentioned results of Shofner and Young (1987). Injections of lidocaine into the AVCN reduce inhibitory inputs to type IV units. The removal of inhibition can be seen as an increase of excitatory rate at frequencies centered around the UER, which lies between the CIA and UIS. Because of our lack of information, the UIS is shown as a single simple input in the schematic of Fig. 15.

Sources of inhibitory inputs in DCN

Inputs accounting for the CIA (i.e., type II units) are thought to be intrinsic to the DCN and probably are the vertical cells (also called corn cells, Lorente de Nô 1981; tuberculoventral cells, Oertel and Wu 1989; or small elongate cells, Brawer et al. 1974) of the deep layer of the DCN. Type II units are found in this layer (Young and Voigt 1982) and can be antidromically activated from axon collaterals in the AVCN (Young 1980), where vertical cells send an axon collateral (Lorente de Nô 1981; Saint Marie et al. 1991). Horseradish peroxidase labeling in rodent CN slices (Oertel and Wu 1989) and Golgi stains (Lorente de Nô 1981) indicate that axonal domains of vertical cells are distributed within an isofrequency sheet and that the cells are able to innervate neurons in both the pyramidal cell and deep layers.

Other inhibitory inputs to type IV cells are more difficult to identify, although possible substrates have been suggested by the use of anatomic techniques. Immunocytochemical techniques have revealed that cartwheel, stellate, and Golgi cells of the superficial DCN stain for γ -aminobutyric acid (GABA) and glycine transmitter systems (Mugnaini 1985; Osen et al. 1990; Saint Marie et al. 1991). Cartwheel cells have been shown to project onto pyramidal cells (Berrebi and Mugnaini 1991; Mugnaini 1985). Cartwheel cells receive excitatory input from granule cells (Wouterlood and Mugnaini 1984), so it is unclear just how frequency specific their activity is. No recordings have been associated with these cells *in vivo*, so it is not known whether they would be activated by the tones used to construct the response maps. These cells constitute important inhibitory connections within the DCN, but their role in generating the responses we measured is unclear. Similar comments apply to stellate cells of the superficial DCN (Wouterlood et al. 1984). Also, one type of stellate cell in the PVCN, the axon of which gives inhibitory terminals, sends an axon collateral to the DCN (Oertel et al. 1990; Smith and Rhode 1989).

Extrinsic inputs could also account for high-frequency inhibitory inputs (UIS) to type IV cells. Horseradish peroxidase application to the cut ends of acoustic stria fibers reveals fibers thought to represent descending inputs to the DCN (Adams and Warr 1976). Retrograde labeling of cell bodies reveals that the origins of some of these fibers are in periolivary cell groups or the contralateral cochlear nu-

cleus. A class of elongate cells in the deep DCN along the stria margin projects to the contralateral DCN (Adams and Warr 1976; Cant and Gaston 1982), although the details of this projection are unclear because the fiber trajectories described by these two authors are different. These elongate cells may be the same as one reported to stain for GABA (Adams and Mugnaini 1987). Although these cells may provide important inputs to the DCN, it is unclear whether their effects would be observed in response maps generated with the use of ipsilateral stimuli only. Additional descending inputs enter the DCN through the centrifugal bundle of Lorente de Nô (1981). One of these inputs originates in the lateral nucleus of the trapezoid body (LNTB), where neurons stain for GABA and project into all CN subdivisions (Spangler et al. 1987; Thompson et al. 1985).

Integration of information across frequency in DCN type IV units

The results in Figs. 11, 12, and 14 are consistent with results reported previously (Young and Brownell 1976; Young 1984) in showing that energy reaching the ear is integrated in a nonlinear fashion by type IV units. Although most of the properties of responses of type IV units to complex stimuli can be accounted for by the properties of type II units (see BBN and notch noise responses), the failure of response maps and quasilinear energy summation as a predictive tool implies that more sophisticated methods will have to be developed for the characterization of complex neural systems like the DCN. An interesting question is whether filter functions derived from rate-versus-cutoff-frequency data would do better at predicting the responses of type IV units to complex stimuli. A filter function can be derived from the first derivative of rate-versus-cutoff-frequency data (Patterson 1976). Use of this filter function would still involve quasilinear energy summation (i.e., a linear summation like Eq. 1), but it might be that a filter function derived with the use of broadband stimuli would be more predictive of responses to similar broadband stimuli than one derived with the use of tones (i.e., the response map). Filter functions could be derived from the rate-versus-cutoff-frequency functions shown in Figs. 11–14. However, such functions are unlikely to be instructive because we used a notch noise protocol that averages together the filtering above and below BF. The response maps of type IV units strongly suggest that filter functions derived from them are asymmetric around BF. To compute such filter functions, it would be necessary to obtain separately responses to the upper and lower passbands of stimuli like ours. Although it may be worthwhile to compute filter functions for DCN units, it seems likely that the quasilinear energy summation model implied by any such filter function will turn out to be inadequate; methods based on nonlinear system theory may be more useful (Aertsen and Johannesma 1981; Backoff and Clopton 1989; Eggermont et al. 1983) and should be investigated further in the DCN.

BBN and notch noise responses

The discrepancy between the excitatory response to BBN and the large inhibitory regions of the type IV response map

CIA is particularly clear for the response map in Fig. 11, which consists only of inhibitory regions over a 30- to 40-dB range of sound levels. We have previously argued that this discrepancy can be explained by the fact that the type II units responsible for the CIA are not activated by broadband stimuli (Young and Brownell 1976; Young and Voigt 1982). Because type II units don't respond to broadband stimuli, they must have strong inhibitory sidebands. However, little is known about the inhibitory inputs to type II cells because these units lack spontaneous activity, so inhibitory areas cannot be demonstrated with single-tone stimuli. By activating a type II unit with a low-level BF tone, it is possible to produce sufficient response to allow the demonstration of inhibitory sidebands with a second tone. Figure 16 shows an example of the result of such an experiment. This type II unit is typical of 11/13 such units studied to date in that it has a clear and strong UIS that is more prominent and of lower threshold than the lower inhibitory sideband. Details of type II response maps and problems of interpretation that arise in two-tone experiments because of the possibility that the apparent inhibition is caused by peripheral two-tone suppression will be discussed elsewhere.

The use of notch noise sheds some light on the transition in type IV units from an excitatory response to BBN to an inhibitory response to narrowband signals such as BF tones. Removing stimulus energy from frequencies in the vicinity of BF causes a reduction in rate, and the notch noise response becomes maximally inhibitory when the notch width is slightly wider than the BFER. The rate reduction undoubtedly reflects removal of excitatory drive from the type IV unit. However, this effect is not sufficient to explain inhibition of the unit by notch noise. An inhibitory input must also be activated by the notch noise.

Because type II units give weak responses to BBN (Young and Brownell 1976; Young and Voigt 1982), they

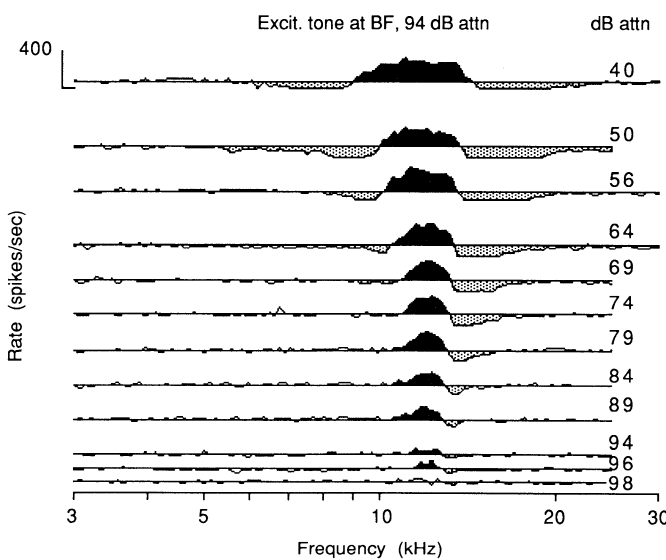


FIG. 16. Response map of a type II unit, measured by use of a 2-tone paradigm. Excitor tone was held constant at BF, a few decibels above threshold; the 2nd tone was varied to generate the response map. Format is otherwise the same as for type IV response maps. BF 12.3 kHz, spont rate 0 spikes/s.

do not appear to be likely candidates to mediate the inhibition by notch noise. However, the convergence of type II units that have a range of BFs onto a type IV unit, and the tuning of CIAs below the type IV BF, make the situation more complicated. Some type II units may be activated by the passband of the notch noise while the notch is located over their prominent UISs, resulting in a net excitatory drive on those type II units and a strong inhibitory input to type IV units that they innervate. The positioning of the UIS in the type II unit in Fig. 16 is precisely what is required to make this idea work.

Alternatively, units that respond weakly to tonal stimuli and therefore are not evident in the response maps, but that respond strongly to broadband stimuli, could confound this interpretation. No such unit type has been isolated so far, either in the DCN (Evans and Nelson 1973a; Shofner and Young 1985; Young and Brownell 1976; Young and Voigt 1982) or in periolivary cell groups projecting to the DCN (Guinan et al. 1972a,b; Tsuchitani 1977). Whether such units exist in the PVCN is not clear. Note that units with this characteristic would be ideal candidates as sources of inhibitory input to type II units.

There are a number of interesting functional implications of the organization of type IV response maps, as summarized in Fig. 15. One consequence of a shift in type II inhibitory BF relative to type IV excitatory BF could be that type IV units are preferentially sensitive to frequency sweeps of a particular direction. Such directional sensitivity has not been found consistently in pyramidal cells of anesthetized cats (Rhode et al. 1983; Smith and Rhode 1985), but in these preparations the inhibition provided by type II inputs is weakened (Evans and Nelson 1973a; Young and Brownell 1976). Another possibility is that tuning of type II inputs below type IV BF could make the local network more sensitive to certain spectral features. One example is sensitivity to the position in frequency of a narrow spectral notch. For notch noises centered below the type IV BF, type II units would be poorly driven because their BFs are in the stopband, but the type IV unit would be strongly driven because its BF is in the passband. The net result would be strong activation of the type IV unit. For notch noises centered on the type IV BF, type II units would be moderately driven because the stopband is located over the dominant part of their UIS, and type IV units would be poorly driven because their BFs are in the stopband. The net result would be inhibition of the type IV unit. Therefore the movement of a spectral notch over the narrow frequency range just described would shift the type IV response from being strongly excitatory to strongly inhibitory. This hypothesis seems to be supported by data in preliminary experiments and suggests a functional role for these cells in the detection of spectral shape cues, such as may be used for monaural sound localization (Musicant et al. 1990; Rice, 1989).

The authors thank colleagues at the Center for Hearing Science for helpful discussions and review of the manuscript and appreciate the comments of the reviewers of the *Journal of Neurophysiology*. We also thank P. Taylor for the histological preparations.

This work was supported by National Institutes of Health Grant R01 DC00115.

Address for reprint requests: G. A. Spirou, Dept. of Biomedical Engineering, Room 506 Traylor Bldg., The Johns Hopkins University School of Medicine, 720 Rutland Ave., Baltimore, MD 21205.

Received 30 October 1990; accepted in final form 13 June 1991.

REFERENCES

- ADAMS, J. C. AND MUGNAINI, E. Patterns of glutamate decarboxylase immunostaining in the feline cochlear nuclear complex studied with silver enhancement and electron microscopy. *J. Comp. Neurol.* 262: 375–401, 1987.
- ADAMS, J. C. AND WARR, W. B. Origins of axons in the cat's acoustic striae determined by injection of horseradish peroxidase into severed tracts. *J. Comp. Neurol.* 170: 107–122, 1976.
- AERTSEN, A. M. H. J. AND JOHANNESMA, P. I. M. The spectro-temporal receptive field. *Biol. Cybern.* 42: 133–143, 1981.
- BACKOFF, P. M. AND CLOPTON, B. M. A time-frequency analysis of DCN and VCN unit responses to wideband noise (Abstract). *Assoc. Res. Otolaryngology Midwinter Meeting* 12: 57, 1989.
- BERREBI, A. S. AND MUGNAINI, E. Distribution and targets of the cartwheel cell axon in the guinea pig dorsal cochlear nucleus. *Anat. Embryol.* 183: 427–454, 1991.
- BLACKSTAD, T. W., OSEN, K. K., AND MUGNAINI, E. Pyramidal neurones of the dorsal cochlear nucleus: a Golgi and computer reconstruction study in cat. *Neuroscience* 13: 827–854, 1984.
- BRAWER, J. R., MOREST, D. K., AND KANE, E. C. The neuronal architecture of the cochlear nucleus of the cat. *J. Comp. Neurol.* 155: 251–300, 1974.
- CANT, N. B. AND GASTON, K. C. Pathways connecting the right and left cochlear nuclei. *J. Comp. Neurol.* 212: 313–326, 1982.
- CANT, N. B. AND MOREST, D. K. The structural basis for stimulus coding in the cochlear nucleus of the cat. In: *Hearing Science. Recent Advances*, edited by C. I. Berlin. San Diego, CA: College Hill, 1984, p. 371–421.
- COHEN, E. C., BRAWER, J. R., AND MOREST, D. K. Projections of the cochlea to the dorsal cochlear nucleus in the cat. *Exp. Neurol.* 35: 450–459, 1972.
- EGGERMONT, J. J., AERTSEN, A. M. H. J., AND JOHANNESMA, P. I. M. Prediction of the responses of auditory neurons in the midbrain of the grass frog based on the spectro-temporal receptive field. *Hearing Res.* 10: 191–202, 1983.
- EVANS, E. F. AND NELSON, P. G. The responses of single neurones in the cochlear nucleus of the cat as a function of their location and the anaesthetic state. *Exp. Brain Res.* 17: 412–427, 1973a.
- EVANS, E. F. AND NELSON, P. G. On the functional relationship between the dorsal and ventral divisions of the cochlear nucleus of the cat. *Exp. Brain Res.* 17: 428–442, 1973b.
- GODFREY, D. A., KIANG, N. Y. S., AND NORRIS, B. E. Single unit activity in the dorsal cochlear nucleus of the cat. *J. Comp. Neurol.* 162: 269–284, 1975.
- GREENWOOD, D. D. AND MARUYAMA, N. Excitatory and inhibitory response areas of auditory neurons in the cochlear nucleus. *J. Neurophysiol.* 28: 863–892, 1965.
- GUINAN, J. J., GUINAN, S. S., AND NORRIS, B. E. Single auditory units in the superior olivary complex. I. Responses to sounds and classifications based on physiological properties. *Int. J. Neurosci.* 4: 101–120, 1972a.
- GUINAN, J. J., NORRIS, B. E., AND GUINAN, S. S. Single auditory units in the superior olivary complex. II. Locations of unit categories and tonotopic organization. *Int. J. Neurosci.* 4: 147–166, 1972b.
- HIRSCH, J. A. AND OERTEL, D. Synaptic connections in the dorsal cochlear nucleus of mice, *in vitro*. *J. Physiol. Lond.* 396: 549–562, 1988.
- JONES, D. R. AND CASSEDAY, J. H. Projections of auditory nerve in the cat as seen by anterograde transport methods. *Neuroscience* 4: 1299–1313, 1979.
- KANE, E. C. Synaptic organization in the dorsal cochlear nucleus of the cat: a light and electron microscopic study. *J. Comp. Neurol.* 155: 301–329, 1974.
- KIANG, N. Y.-S. AND MOXON, E. C. Tails of tuning curves of auditory-nerve fibers. *J. Acoust. Soc. Am.* 55: 620–630, 1974.
- LORENTE DE NÓ, R. *The Primary Acoustic Nuclei*. New York: Raven, 1981.
- MANIS, P. B. Responses to parallel fiber stimulation in the guinea pig dorsal cochlear nucleus *in vitro*. *J. Neurophysiol.* 61: 149–161, 1989.
- MANIS, P. B. AND BROWNELL, W. E. Synaptic organization of eighth nerve afferents to the cat dorsal cochlear nucleus. *J. Neurophysiol.* 50: 1156–1181, 1983.
- MUGNAINI, E. GABA neurons in the superficial layers of rat dorsal cochlear nucleus: light and electron microscopic immunocytochemistry. *J. Comp. Neurol.* 235: 61–81, 1985.
- MUGNAINI, E., OSEN, K. K., DAHL, A.-L., FRIEDRICH, V. L., AND KORTE, G. Fine structure of granule cells and related interneurons (termed Golgi cells) in the cochlear nuclear complex of cat, rat and mouse. *J. Neurocytol.* 9: 537–570, 1980a.
- MUGNAINI, E., WARR, W. B., AND OSEN, K. K. Distribution and light microscopic features of granule cells in the cochlear nuclei of cat, rat and mouse. *J. Comp. Neurol.* 191: 581–606, 1980b.
- MUSICANT, A. D., CHAN, J. C. K., AND HIND, J. E. Directional dependent properties of cat external ear: new data and cross-species comparisons. *J. Acoust. Soc. Am.* 87: 757–781, 1990.
- OERTEL, D. AND WU, S. H. Morphology and physiology of cells in slice preparations of the dorsal cochlear nucleus of mice. *J. Comp. Neurol.* 283: 228–247, 1989.
- OERTEL, D., WU, S. H., GARB, M. W., AND DIZACK, C. Morphology and physiology of cells in slice preparations of the posteroventral cochlear nucleus of mice. *J. Comp. Neurol.* 295: 136–154, 1990.
- OSEN, K. K. Cytoarchitecture of the cochlear nuclei in the cat. *J. Comp. Neurol.* 136: 454–483, 1969.
- OSEN, K. K. Course and termination of the primary afferents in the cochlear nuclei of the cat, an experimental anatomical study. *Arch. Ital. Biol.* 108: 21–51, 1970.
- OSEN, K. K., OTTERSEN, O. P., AND STORM-MATHISEN, J. Colocalization of glycine-like and GABA-like immunoreactivities. A semiquantitative study of individual neurons in the dorsal cochlear nucleus of cat. In: *Glycine Neurotransmission*, edited by O. P. Ottersen and J. Storm-Mathisen. New York: Wiley, 1990, p. 417–451.
- PATTERSON, R. D. Auditory filter shapes derived with noise stimuli. *J. Acoust. Soc. Am.* 59: 640–654, 1976.
- RAMÓN Y CAJAL, S. *Histologie du système nerveux de l'homme et des vertébrés*. Madrid: Instituto Ramón y Cajal, 1909 (1952 reprint).
- RHODE, W. S. AND KETTNER, R. E. Physiological study of neurons in the dorsal and posteroventral cochlear nucleus of the unanesthetized cat. *J. Neurophysiol.* 57: 414–442, 1987.
- RHODE, W. S. AND SMITH, P. H. Physiological studies of neurons in the dorsal cochlear nucleus of cat. *J. Neurophysiol.* 56: 287–307, 1986.
- RHODE, W. S., SMITH, P. H., AND OERTEL, D. Physiological response properties of cells labeled intracellularly with horseradish peroxidase in cat dorsal cochlear nucleus. *J. Comp. Neurol.* 213: 426–447, 1983.
- RICE, J. J. *Free Field to Eardrum Pressure Transformations in Cats* (Masters thesis). Baltimore, MD: The Johns Hopkins University, 1989.
- SAINT MARIE, R. L., BENSON, C. G., OSTAPOFF, E. M., AND MOREST, D. K. Glycine immunoreactive projection from the dorsal to the anteroventral cochlear nucleus. *Hearing Res.* 51: 11–28, 1991.
- SHOFNER, W. P. AND YOUNG, E. D. Excitatory/inhibitory response types in the cochlear nucleus: relationships to discharge patterns and responses to electrical stimulation of the auditory nerve. *J. Neurophysiol.* 54: 917–939, 1985.
- SHOFNER, W. P. AND YOUNG, E. D. Inhibitory connections between AVCN and DCN: evidence from lidocaine injection in AVCN. *Hearing Res.* 29: 45–53, 1987.
- SMITH, P. H. AND RHODE, W. S. Electron microscopic features of physiologically characterized, HRP-labeled fusiform cells in the cat dorsal cochlear nucleus. *J. Comp. Neurol.* 237: 127–143, 1985.
- SMITH, P. H. AND RHODE, W. S. Structural and functional properties distinguish two types of multipolar cells in the ventral cochlear nucleus. *J. Comp. Neurol.* 282: 595–616, 1989.
- SOKOLICH, W. G. Improved acoustic system for auditory research (Abstract). *J. Acoust. Soc. Am.* 62: S12, 1977.
- SPANGLER, K. M., CANT, N. B., HENKEL, C. K., FARLEY, G. R., AND WARR, W. B. Descending projections from the superior olivary complex to the cochlear nucleus of the cat. *J. Comp. Neurol.* 259: 452–465, 1987.
- THOMPSON, G. C., CORTEZ, A. M., AND LAM, D. M.-K. Localization of GABA immunoreactivity in the auditory brainstem of guinea pigs. *Brain Res.* 339: 119–122, 1985.
- TSUCHITANI, C. Functional organization of lateral cell groups of cat superior olivary complex. *J. Neurophysiol.* 40: 296–318, 1977.
- VOIGT, H. F. AND YOUNG, E. D. Evidence of inhibitory interactions be-

- tween neurons in the dorsal cochlear nucleus. *J. Neurophysiol.* 44: 76-96, 1980.
- VOIGT, H. F. AND YOUNG, E. D. Cross-correlation analysis of inhibitory interactions in dorsal cochlear nucleus. *J. Neurophysiol.* 64: 1590-1610, 1990.
- WARR, W. B. Parallel ascending pathways from the cochlear nucleus: neuroanatomical evidence of functional specialization. *Contrib. Sens. Physiol.* 7: 1-38, 1982.
- WICKESBERG, R. E. AND OERTEL, D. Tonotopic projection from the dorsal to the anteroventral cochlear nucleus of mice. *J. Comp. Neurol.* 268: 389-399, 1988.
- WICKESBERG, R. E. AND OERTEL, D. Delayed, frequency-specific inhibition in the cochlear nuclei of mice: a mechanism for monaural echo suppression. *J. Neurosci.* 10: 1762-1768, 1990.
- WOUTERLOOD, F. G. AND MUGNAINI, E. Cartwheel neurons of the dorsal cochlear nucleus: a Golgi-electron microscopic study in rat. *J. Comp. Neurol.* 227: 136-157, 1984.
- WOUTERLOOD, F. G., MUGNAINI, E., OSSEN, K. K., AND DAHL, A.-L. Stellate neurons in rat dorsal cochlear nucleus studied with combined Golgi impregnation and electron microscopy: synaptic connections and mutual coupling by gap junctions. *J. Neurocytol.* 13: 639-664, 1984.
- YOUNG, E. D. Identification of response properties of ascending axons from dorsal cochlear nucleus. *Brain Res.* 200: 23-38, 1980.
- YOUNG, E. D. Response characteristics of neurons of the cochlear nuclei. In: *Hearing Science. Recent Advances*, edited by C. I. Berlin. San Diego, CA: College Hill, 1984, p. 423-460.
- YOUNG, E. D. AND BROWNELL, W. E. Responses to tones and noise of single cells in dorsal cochlear nucleus of unanesthetized cats. *J. Neurophysiol.* 39: 282-300, 1976.
- YOUNG, E. D. AND VOIGT, H. F. The internal organization of the dorsal cochlear nucleus. In: *Neuronal Mechanisms in Hearing*, edited by J. Syka and L. Aitkin. New York: Plenum, 1981, p. 127-133.
- YOUNG, E. D. AND VOIGT, H. F. Response properties of type II and type III units in dorsal cochlear nucleus. *Hearing Res.* 6: 153-169, 1982.